Performance of hydrophobic physical solvents for pre-combustion CO_2 capture at a pilot scale coal gasification facility

Kathryn H. Smith [a], Husain E. Ashkanani [d], Robert L. Thompson [a], Jeffrey T. Culp [a], Lei Hong [a], Mike Swanson [b], Joshua Stanislowski [b], Wei Shi [a], Badie I. Morsi [a,c], Kevin Resnik [a], David P. Hopkinson [a], Nicholas S. Siefert [a,*]

[a] U.S. Department of Energy, National Energy Technology Laboratory, P.O. Box 10940, Pittsburgh, PA 15236, USA

[b] Energy & Environmental Research Center, University of North Dakota, Grand Forks, ND, USA

[c] Department of Chemical and Petroleum Engineering, University of Pittsburgh, Pittsburgh, PA 15261, USA

[d] Chemical Engineering Department, Kuwait University, P.O. Box 5969, 13060, Kuwait

[*] Corresponding Author: Nicholas.Siefert@netl.doe.gov

Abstract

Here, we present the first pilot plant data for hydrophobic physical solvents for CO_2 and H_2S removal from coal-derived H_2-rich syngas. Four physical solvents were tested under pre-combustion CO_2 capture conditions at bench scale and pilot plant scale: one baseline hydrophilic solvent and three hydrophobic solvents. The solvents were: (1) polyethylene-glycol-dimethyl ether (PEGDME), a hydrophilic solvent analog for the commercial process Selexol, (2) tributyl-phosphate (TBP), a commercially available hydrophobic solvent, (3) polyethylene glycol-poly(dimethylsiloxane) (PEG-PDMS-3), and (4) diethyl sebacate (CASSH-1), a novel, computationally screened hydrophobic solvent developed by the National Energy Technology Laboratory (NETL). All solvents were studied under pure gas (CO_2/N_2/H_2/CH_4) equilibrium conditions at NETL followed by pilot plant testing with syngas at the University of North Dakota Energy & Environmental Research Center (UND EERC). Long term performance of CASSH-1

and PEDGME was then assessed with results compared to process simulation predictions. Within experimental uncertainties, all solvents showed comparable CO_2 absorption performance at above room temperature operation while the hydrophobic solvents had limited water uptake and low vapor pressure, which alleviates concerns related to corrosion, water absorption, and solvent loss to evaporation. These results indicate low viscosity, low vapor pressure hydrophobic solvents are a promising option for lower cost CO_2 capture from high pressure syngas applications.

Keywords: pre-combustion, CO_2 capture, carbon dioxide, CO_2, hydrogen, H_2, pilot plant, gas absorption, physical solvent, hydrophobic solvent, vapor liquid equilibrium, process simulation

1 Introduction

Pre-combustion CO_2 capture processes are becoming increasingly important for the rapidly developing clean or blue hydrogen industry and have potential to significantly reduce greenhouse gas emissions in power generation, transportation, and industrial sectors (Global CCS Institute, 2021). Clean or 'blue hydrogen' refers to hydrogen produced from fossil fuels, including steam methane reforming (SMR) from natural gas or gasification from a solid fuel like coal, with CO_2 capture and storage (Global CCS Institute, 2021; Lau et al., 2021). Due to the high partial pressure of carbon dioxide (CO_2) in these applications, pre-combustion CO_2 capture can be achieved through inexpensive physical solvents where acid gases (CO_2 and H_2S) dissolve into the solvent while the desired fuel product (H_2) and potential corrosion enabler (H_2O) can be kept out of the solvent by choosing optimal solvent functional groups. An example of where pre-combustion CO_2 capture could be applied is at an integrated gasification combined cycle (IGCC) power plant which utilizes heat, steam and/or oxygen under pressure in a gasifier to convert solid fuels like coal into a synthetic gas (syngas) that can be used to generate power. The syngas exiting the gasifier is at high pressure and contains mainly carbon monoxide (CO) and hydrogen (H_2) along with other components like CO_2 and methane (CH_4). For IGCC with pre-combustion CO_2 capture, a water gas shift (WGS) reactor is typically used to convert CO in the syngas into CO_2 and more H_2 through reaction with H_2O. The syngas exiting the WGS reactor now has a high partial pressure of CO_2 which makes physical solvent absorption an ideal option for CO_2 capture from the H_2 rich syngas.

Solvent absorption processes have been used for many years to separate acid gases like H_2S and CO_2 from high pressure fuel gas streams (Kohl and Nielsen, 1997). Some of these

processes operate with chemical solvents like MDEA (Moioli et al., 2014) or potassium carbonate (Smith et al., 2012), but in general, non-reacting physical solvents are thought to be the most economical option for bulk acid gas removal from high pressure syngas streams (Mumford et al., 2015; Smith et al., 2022), particularly if the goal is to desorb the acid gases at high pressure rather than vent to the atmosphere. A number of commercial physical solvent gas absorption processes are available including the Selexol (Honeywell UOP) and Rectisol (Air Liquide) processes which can both remove H_2S and CO_2 (Kohl and Nielsen, 1997). The Rectisol process uses methanol as its solvent and operates at an extremely low absorption temperature (around -50°C) which requires an energy intensive refrigeration system. The main advantage of the Rectisol process is that it can remove all undesirable components including H_2S, COS and CO_2 in the same process, and in particular, it can remove H_2S to very low levels (Koytsoumpa et al., 2015). The Selexol process uses a solvent containing a mixture of dimethyl ethers of polyethylene glycol and has several benefits including high CO_2/H_2 selectivity, low solvent cost, and low vapor pressure compared with methanol. However, due to their operation below room temperature, both the Selexol and the Rectisol processes have the disadvantages of significant cooling duties and the inability to efficiently make use of waste heat for operation above room temperature. If solvent regeneration were to occur at higher pressure using a temperature swing process (rather than traditional pressure swing), then waste heat from the plant could be used to efficiently regenerate the solvent while also producing a higher-pressure CO_2 product stream suitable for transportation in CO_2 pipelines.

Most commercial physical solvent absorption processes, like Selexol and Rectisol, use hydrophilic solvents that were originally developed for the treatment of natural gas streams at ambient temperatures where acid gases (like CO_2 and H_2S) and water vapor both need to be removed prior to injection into a natural gas pipeline. For acid gas removal (AGR) at room temperature or below room temperature prior to entry into a pipeline, hydrophilic solvents can be used to meet natural gas pipeline specifications while minimizing absorption of fuel into the solvent. However, in most cases, the absorbed gases are flared and vented. Before greenhouse gas (GHG) credits/taxes, there was no incentive to regenerate CO_2 at high pressure. Now with GHG credits/taxes through the global market, new solvents and solvent processes are needed to capture CO_2 and efficiently regenerate the CO_2 at high partial pressure to minimize compression costs.

For pre-combustion CO_2 capture at an IGCC plant, syngas enters the absorption process at a much higher temperature compared to AGR from natural gas processing, resulting in the need

for significant syngas cooling if traditional hydrophilic physical solvent processes are to be used for CO_2 removal. If the pre-combustion CO_2 capture solvent absorption process could be operated at higher temperature and pressure, the overall thermal efficiency of the power plant would be improved. In addition to issues with solvent water miscibility, other challenges associated with commercially available hydrophilic physical solvents for pre-combustion CO_2 capture include high vapor pressure, high viscosity after absorbing water from the gas stream, high corrosion potential and the need for solvent regeneration by pressure reduction resulting in a low pressure CO_2 product stream that will require further costly compression before geological storage or use in other applications like enhanced oil recovery (EOR). In addition, water vapor must be separated from the CO_2 gas stream after solvent regeneration, which leads to an additional cost for CO_2 capture. If the solvent regeneration process were to occur at higher pressures using waste or low-grade heat, further energy and cost advantages would be realized (Li et al., 2015; Siefert and Hopkinson, 2018; Siefert et al., 2016a; Siefert et al., 2016b).

It was with these challenges that hydrophobic physical solvents were proposed for CO_2 capture from high pressure syngas streams (Enick et al., 2013; Shi et al., 2016; Shi et al., 2015; Siefert et al., 2016b; Smith et al., 2022; Thompson et al., 2019). Ideal properties of a hydrophobic physical solvent include high thermal stability, low corrosion, low cost, high CO_2 absorption capacity, low H_2 uptake, low vapor pressure, low viscosity, non-foaming and non-toxic. A number of hydrophobic physical solvents have been investigated at bench scale for CO_2 absorption. Some of these solvents, e.g. polydimethylsiloxane (PDMS), have advantages such as non-absorption of water but showed low CO_2/H_2 selectivity (Enick et al., 2013; Shi et al., 2016). Other solvents were found to have properties that would limit industrial application, such as poly(propylene glycol) di-methyl ether (PPGDME) which formed a gel in the presence of water and polyethylene glycol (PEG)-siloxane solvent (PEG-PDMS-1) which suffered from foaming (Thompson et al., 2019). Further R&D on the PEG-siloxane based solvents led to the development of polyethylene glycol-poly(dimethylsiloxane) (PEG-PDMS-3) which avoided foaming issues while still providing high CO_2/H_2 selectivity at above room temperature conditions at bench scale (CO_2/H_2 selectivity of ~70 at 25°C and ~60 at 40°C) (Siefert and Hopkinson, 2018). Subsequently, a computational screening study by NETL showed that the hydrophobic solvent diethyl sebacate, termed CASSH-1 (Computationally Assisted Screened Solvent Hydrophobic-1,) had absorption capacity and selectivity comparable to Selexol and PEG-PDMS-3, but with no foaming issues and very low

vapor pressure (Shi et al., 2018; Shi et al., 2021). Although these computational screening and bench scale experimental studies using hydrophobic physical solvents have shown promising CO_2 absorption performance, none of these solvents have been tested under process conditions with real syngas to fully assess their potential for CO_2 capture at industrial scale.

To date in the engineering literature, there has been some, but limited, pilot plant testing of pre-combustion CO_2 capture from real syngas using solvent absorption processes. The Estasolvan process, which uses the solvent tributyl phosphate (TBP), has not been applied commercially but has shown potential as a physical solvent under pilot plant conditions for H_2S absorption (Bucklin and Schendel, 1984; Franckwiak and Nitschke, 1970; Newman, 1985). Pre-combustion CO_2 capture from a research scale coal-based gasification process has been demonstrated in Australia using a pilot plant with the chemical solvent potassium carbonate, which showed that minor syngas components can impact solvent physical properties and subsequently absorption column performance (Smith et al., 2009; Smith et al., 2012). The United States Department of Energy (US DOE) established the National Carbon Capture Center (NCCC) to test emerging CO_2 capture technologies including pre-combustion capture using a coal based IGCC process (Morton et al., 2013). Gasification and pre-combustion capture processes were tested from 2011 until 2017 after which the facility exclusively tested under post-combustion conditions using both coal and natural gas boilers. During the pre-combustion testing period, well-known chemical and physical solvents such as ammonia, potassium carbonate, potassium prolinate, alkylimidazoles and dimethyl ether of polyethylene glycol (PEGDME) were tested for CO_2 absorption characteristics, co-absorption of H_2S, regeneration characteristics and performance in the presence of water (Nagar et al., 2017; Wu, 2022). A pre-combustion CO_2 capture pilot plant at the Buggenum IGCC in The Netherlands has also been used to test the performance of the hydrophilic physical solvent PEGDME (Damen et al., 2011; Trapp et al., 2015a; Trapp et al., 2015b). To date, there have not been any known industrial demonstrations or pilot plant trials using hydrophobic physical solvents for pre-combustion CO_2 capture from coal derived syngas.

Therefore, the objectives of this study were to: (1) measure the physical properties and vapor liquid equilibrium (VLE) data of selected hydrophobic physical solvents using bench scale equipment with pure gas; (2) extend testing of these hydrophobic physical solvents to short and long term pilot plant testing using coal derived syngas, (3) to compare hydrophobic solvent performance against a baseline hydrophilic physical solvent, and finally (4) regress bench-scale

pure gas VLE data into process simulations to predict the pilot plant performance. The pure gas VLE conditions for the selected physical solvents were measured with CO_2, H_2, N_2 and CH_4. Pilot plant testing was then performed with the commercially-available hydrophilic physical solvent PEGDME (Selexol surrogate) to establish a mixed-gas process performance baseline which was followed by testing of three hydrophobic physical solvents: CASSH-1, PEG-PDMS-3 and TBP. All four solvents were initially tested over a range of operating conditions (varying temperature and solvent flow rates) using coal derived syngas produced from the pilot scale IGCC power plant at University of North Dakota Energy & Environmental Research Center (UND EERC). This was followed by an assessment of longer-term absorption performance in the pilot plant using the solvents CASSH-1 and PEGDME at constant operating conditions. Finally, the performance data obtained from the longer-term pilot plant operation were used with VLE data for development and validation of a process simulation.

2 Materials & Methods

2.1 Physical solvents – PEGDME, CASSH-1, PEG-PDMS-3, TBP.

Four physical solvents have been tested for CO_2 removal from syngas operated under pre-combustion CO_2 capture conditions. A surrogate to the commercially available hydrophilic solvent used in the Selexol process, called PEGDME, was used to develop a performance baseline followed by testing of the hydrophobic solvents: CASSH-1, PEG-PDMS-3 and TBP (Shi et al., 2018; Thompson et al., 2019). PEGDME was obtained from Coastal Chemical Co.; PEG-PDMS-3 was manufactured by Gelest Inc.; TBP was purchased from ThermoFisher Scientific; and CASSH-1 was purchased from Sigma Aldrich.

The first pilot plant trial (Trial #1) was conducted to screen the absorption performance of the four solvents listed in Table 1. Following this screening study, PEGDME and CASSH-1 were tested continuously for 5 days each to assess longer term solvent performance (Trial #2).

Table 1. Physical properties of solvents tested in the pilot plant trials in this study (Shi et al., 2019; Shi et al., 2021; Smith et al., 2022)

Solvent	PEGDME	CASSH-1	PEG-PDMS-3	TBP
Molecular Weight (g mol^{-1})	280	258	620	266
Viscosity @ 25 °C (cP)	5.8	5.1	12.2	2.9
Density @ 25 °C (kg m^{-3})	1030	960	987	979
Vapor pressure @ 25°C (Pa)	0.1	0.07	<0.1	0.15

2.2 Bench Scale VLE Measurements

Two gravimetric gas adsorption systems (Hiden IGA (Intelligent Gravimetric Analysis) and TA Instruments Isosorp) and a continuous stirred tank reactor (CSTR; Autoclave Engineering) were used to measure the VLE data for a range of gases using the four dry physical solvents listed in Table 1. Solvents were dried by heat and vacuum before adding gases to the apparatus. The gases were purchased from Butler Gas Products Company and the purities of CO_2, H_2, N_2 and CH_4 were all 99.99%. There was no further treatment of the gases or the solvents before use. The VLE data were measured at multiple pressures up to 3 MPa and at temperatures including 10, 25, 40 and 55°C. Further detail on the specifications and operating procedures for the CSTR has been described by Siefert et al. (2016b) and further information on the IGA system has been provided by Thompson et al. (2019). The operating procedures for the gravimetric TA Instruments Isosorp gas absorption system are similar to those used for the gravimetric Hiden IGA system as both require buoyancy compensations to account for the effect of gas density on the sample weight. The Isosorp system calculates the gas density in real time using an internal calibrated weight. The sample weight is then corrected for buoyancy forces using the experimental gas density determined from the calibrated weight readings at each pressure step of the isotherm. Additional buoyancy corrections for balance components were determined using the volumes supplied by the instrument vendor. The sample densities were measured independently using a Rudolph Research Analytical

DDM 2911 automated density meter. For CO_2 absorption calculations on both the IGA and Isosorp VLE systems, an additional buoyancy correction was applied to account for an estimated volume expansion of 0.0433 cm^3/mmol CO_2 absorbed in the solvent. The sample size used in the Isosorp system ranges from 0.5 – 1.5g whereas the samples sizes used for the IGA tests were in the range of 0.04-0.1g. The larger sample size and higher pressure range for the Isosorp tests provided a more significant weight change for weakly absorbing gases such as H_2, N_2, and CH_4 and was the gravimetric instrument of choice for these measurements. Absorption measurements on the IGA apparatus were limited to a pressure of 1.8 MPa. The Isosorp measurements were conducted to pressures up to 5 MPa. Experimental absorption isotherms were smoothed using either linear or exponential fits as appropriate. Absorbed amounts of gas were then calculated at regular pressure intervals for tabulation and comparison between solvents. The amount of gas absorbed into the solvent from each VLE apparatus was used to determine the gas solubility and selectivity, at specific temperature and gas partial pressure, as shown in Equations (1) and (2) below.

$$\text{Gas solubility}(mol \cdot L^{-1}) = \frac{\text{gas absorbed into solvent (mol)}}{\text{Lean solvent volume (L)}} \quad (1)$$

$$\text{Selectivity A/B} = \frac{\text{Gas solubility}_{\text{gas A}}\ (mol \cdot L^{-1})}{\text{Gas solubility}_{\text{gas B}}\ (mol \cdot L^{-1})} \quad (2)$$

2.3 Pilot Plant Specifications and Operating Conditions

Two pilot plant trials were conducted at the UND EERC. A fluidized bed gasifier was operated in oxygen-blown mode at a pressure close to 5 MPa using a well characterized lignite from the Center Mine, North Dakota. The coal contained 1 wt% sulfur which provided an H_2S concentration relevant for assessing H_2S absorption performance in addition to CO_2 absorption performance. A sour shift catalyst (TDA Research, Wheat Ridge, CO) was used in the WGS reactor to convert CO to CO_2 and H_2. The two stages of water gas shift were operated at approximately 4.96 MPa (720 psia) with average operating temperatures of 312°C and 249°C with a standard gas hourly space velocity (SGHSV) of approximately 7600 hr^{-1} (at standard conditions of 15.5°C and 14.7 psia). Table 2 is a summary of the average gasifier operating conditions and average syngas composition for the two pilot plant trials. Note that this syngas had a relatively high N_2 content due to the need to positively purge the electronics inside of the pressurized fuel feeder with an inert gas, in this case N_2.

Table 2. Average shifted syngas conditions and composition entering absorber column for each pilot plant trial. (Shifted syngas reported on a dry basis due to analytical equipment requirements). The statistical error is reported as the standard deviation from multiple measurements.

Parameter	**Trial 1**	**Trial 2**
Syngas total pressure, MPa	4.88 ± 0.02	4.86 ± 0.01
Syngas temperature, °C	37.5 ± 0.8	37.6 ± 0.9
Syngas flow rate, std. $m^3 \cdot h^{-1}$	3.8 ± 0.2	3.5 ± 0.1
Syngas composition, dry, avg (mol%)		
CO_2	52.0 ± 1.8	55.4 ± 1.5
H_2	13.1 ± 2.9	15.7 ± 1.3
N_2	32.7 ± 3.7	25.4 ± 2.1
CH_4	1.6 ± 0.7	2.1 ± 0.3
CO	0.2 ± 0.05	1.1 ± 0.4
H_2S	0.5 ± 0.05	0.4 ± 0.05

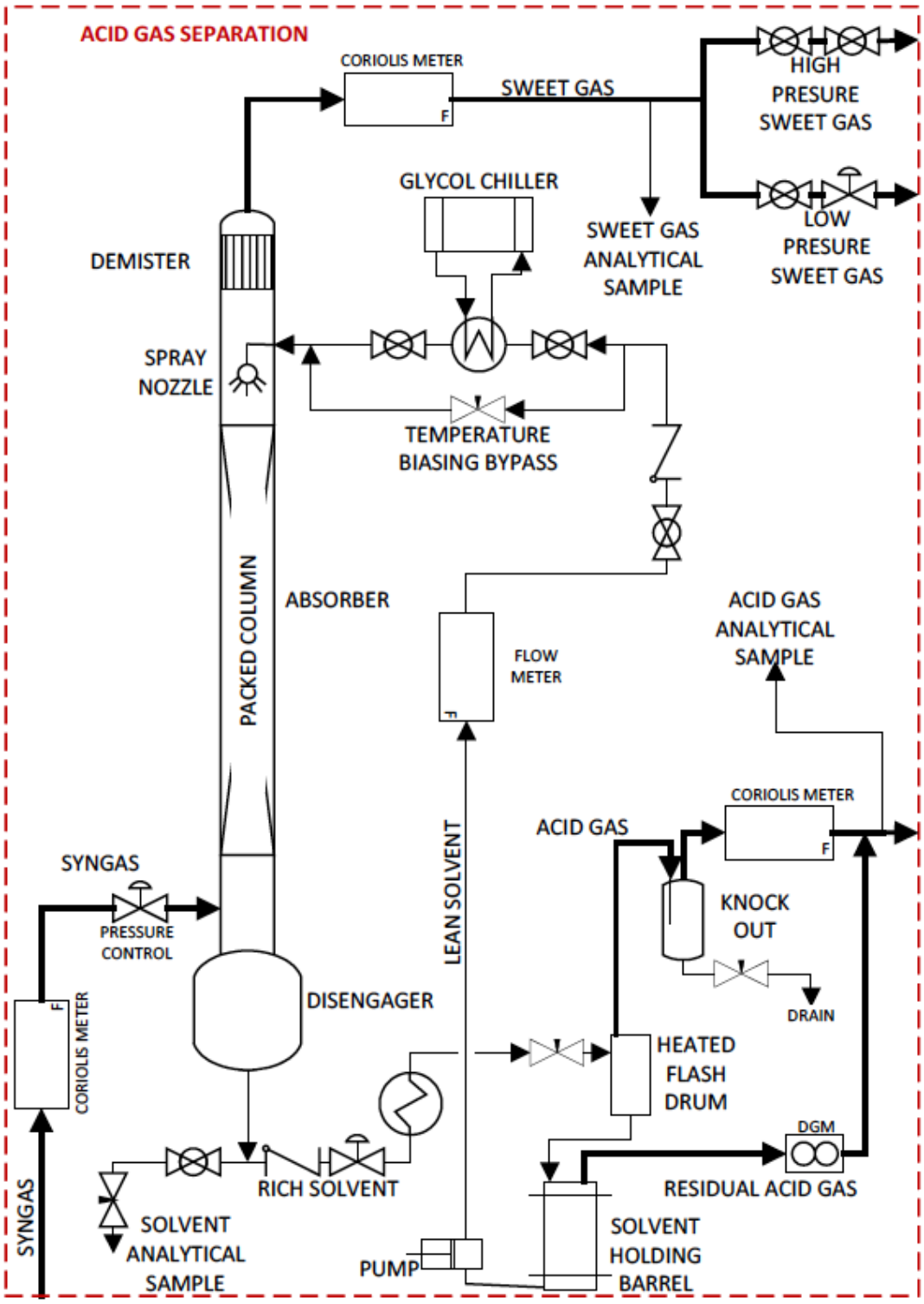

238

239 ***Figure 1. Process flow diagram of CO_2 capture pilot plant at UND EERC***

240

Figure 1 is a process flow diagram of the CO_2 capture pilot plant. The compressed syngas enters the absorption column at a gas flow rate of approximately 3.8 std. $m^3 \cdot h^{-1}$ (or 0.047 $mol \cdot s^{-1}$) and at an absolute pressure of approximately 4.9 MPa. The gas was saturated with water vapor at the syngas inlet temperature of approximately 38°C (~6.6 kPa, or 0.1%vol); however, it should be noted that experimental gas compositions reported throughout this manuscript are reported on a dry basis. The lean solvent entered the top of the absorption column at a controlled temperature between 10 and 55°C, depending on the controlled test conditions. Solvent flowrates varied between 28 and 45 $L \cdot h^{-1}$, depending on the controlled test conditions, with the goal of varying the percentage of CO_2 removal. The absorption column had a diameter of 76.2 mm ID and was filled with 5/8" IMTP15 metal random packing (Koch-Glitsch) with a packed height of 3.2 m. The CO_2 loaded solvent exited the bottom of the absorber and flowed through a level control valve, heat exchanger and flow constrictor (metering valve) and finally to the solvent regeneration in the flash drum. The lean solvent was returned to the absorber via a holding tank, pump, flow meter and heat exchanger. The absorber sweet gas passes through a demister to drop entrained solvent before the gas exits the top of the absorption column.

For the first pilot plant trial (Trial #1, solvent screening), the syngas flow rate was kept constant at approximately 3.8 std. $m^3 \cdot h^{-1}$ (0.047 $mol \cdot s^{-1}$) and solvent flow rates varied between approximately 28 and 45 $L \cdot h^{-1}$ for a range of solvent inlet temperatures including 10, 25, 40 and 55°C (PEGDME was not tested at 55 °C since the Selexol absorption process is typically operated at no more than 38 °C (100 °F) (Cowan et al., 2011)). Changes in operating parameters (i.e., temperature or flow rate) were maintained for at least 2 hours to achieve steady-state conditions. The solvents were regenerated in a single stage flash drum operated at approximately 43°C. The solvent was not cooled before entering the flash drum so regeneration temperature may have been higher than 43°C when the solvent was operated at 55°C in the absorber.

For the second pilot plant trial (Trial #2, long term solvent performance testing, 10 days), the operating conditions remained constant with a syngas flow rate of approximately 3.5 std. $m^3 \cdot h^{-1}$ (0.043 $mol \cdot s^{-1}$) at approximately 38 °C, solvent inlet temperature of 25 °C and solvent flow rate of approximately 32 $L \cdot h^{-1}$. The solvents were regenerated in a single stage flash drum at a temperature of 66 °C, which was approximately 23 °C higher than the first solvent screening trial. During Trial #2, a dry gas meter and a gas analyzer were added to the solvent storage tank to

271 determine if any gasses were being released from the solvent tank in addition to the flash tank.

272 During operation of the pilot plant, the gas composition and gas flow rate were measured
273 simultaneously via online analyzers for the syngas (absorber feed), sweet gas (top of absorber) and
274 acid gas (flash tank gas). Two gas analyzers were present on each gas stream to measure dry gas
275 composition including a Laser Gas Analyzer (LGA, Aerodyne Research, Inc.), which is a high-
276 speed gas spectrometer that measures concentrations of eight or more gases simultaneously and a
277 gas chromatography (GC) analyzer by Varian or Yokogawa for measuring H_2, CO, CO_2, N_2, O_2,
278 H_2S, CH_4 and other hydrocarbons. Analyzer measurement errors were minimized by averaging the
279 gas composition data from the two different gas analyzers present on each gas stream. Statistical
280 error for gas composition data was calculated as the standard deviation (confidence interval, CI =
281 68%). Dräger tubes were also occasionally used to detect the presence of gas components that
282 cannot be detected by the online analyzers, including HCN, NH_3, HCl, benzene, toluene and
283 xylene.

284 The absorption performance of the solvent was assessed by calculating gas removal
285 efficiency (e.g. CO_2 removal efficiency as represented by equation (3)) and gas uptake into the
286 solvent (as represented by equation (4)). The amount of CO_2 absorbed into the solvent (or other
287 gas component like H_2S, H_2, etc.) was determined as an average of two methods: (1) the difference
288 between CO_2 entering and exiting the absorber and (2) the amount of CO_2 removed from the
289 solvent flash/regeneration process. For pilot plant data, both statistical (random fluctuations) and
290 systemic errors (uncertainty from pilot plant equipment calibration, etc.) were calculated for gas
291 uptake into the solvent. Statistical error for gas uptake was calculated as the standard deviation (CI
292 = 68%) from data collected from the two gas analyzers per gas stream and the two methods for
293 determining gas absorption into the solvent. Systemic error, due to uncertainties in pilot plant flow
294 meter calibrations, was estimated to be 6% for all solvents through the use of mass and mole
295 balance checks, which provided secondary checks on reported flow rates. Note that the gas uptake
296 calculated using Eq. (4) is different than the VLE gas uptake. When calculating gas uptake using
297 the pilot scale test data (Eq. 4), there is a thermodynamic driving force for gas absorption from the
298 gas stream to the solvent phase. In contrast, for the VLE experiment to obtain gas uptake, the
299 chemical potentials for all gases are equal between the gas and the solvent phases. To further
300 improve data analysis accuracy, pilot plant data were only analyzed if the gas phase mole balance
301 error was less than 20%.

$$\mathrm{CO_2\ Removal\ Efficiency\ [\%]} = \frac{\mathrm{CO_2\ absorbed\ into\ solvent\ (mol\ \cdot\ hr^{-1})}}{\mathrm{CO_2\ in\ syngas\ (mol\cdot\ hr^{-1})}} \times 100 \quad (3)$$

$$\mathrm{Gas\ Uptake\ into\ solvent\ [mol\cdot L^{-1}]} = \frac{\mathrm{CO_2\ absorbed\ in\ solvent\ (mol\cdot hr^{-1})}}{\mathrm{Solvent\ flow\ rate\ (L\cdot hr^{-1})}} \quad (4)$$

2.4 Process Simulation Development

Aspen Plus version 11 was used to develop process simulations for the pilot plant operation during trial #2 with PEGDME and CASSH-1. The simulation flowsheet is shown in Figure 2 and a summary of the input conditions, which were kept constant in the simulations, can be found in

Table ***3***. The process flow sheet consisted of one absorption tower, one flash tank, one solvent pump, and one heat exchanger. Laboratory measured VLE data were used to validate the thermodynamic properties predicted within Aspen Plus via the Perturbed-Chain Statistical Association Fluid Theory (PC-SAFT) Equation of State (EOS) method. The binary interaction parameters for CO_2, H_2, N_2 and CH_4 were regressed from the experimental VLE data to predict the non-ideal system. Information on the PC-SAFT binary interaction parameters used to predict gas solubility in the solvents can be found in the supplemental information Table S8 and previous studies (Ashkanani et al., 2020). H_2O and H_2S were included in the simulations but experimental VLE data were not used to regress the binary interaction parameters for these components. The physical properties of gas species and solvents were predicted via built-in models within Aspen Plus and validated using experimental data. The gas phase mass transfer resistance was assumed to be negligible, and the absorption rate was assumed to be controlled by mass transfer resistance in the liquid-film. The liquid-phase mass transfer coefficient and effective gas-liquid interfacial area were predicted by Onda's correlations (Onda et al., 1968) which are applicable for the packing materials and physical properties relevant to the current study. Both the rate-based and equilibrium models were used to predict absorber performance via the Aspen RadFrac block without a reboiler. The liquid holdup was predicted using the Billet and Schultes (1993) correlation and absorber flooding and pressure drop (Piché et al., 2001) were predicted by the modified generalized pressure drop correlation by Leva (1992). The shifted syngas entered at the bottom of the absorber and exited at the top while the lean-solvent entered the absorber from the top of the column. The number of stages in the absorber was set to 10 equilibrium stages and 100 stages for the rate-based model. The CO_2-rich solvent leaves the absorber to be regenerated in the flash tank which was modelled as an adiabatic equilibrium SEPARATOR block. A solvent cooler is used to cool the solvent to 25 °C. A summary of the input conditions for the process simulations developed for trial 2 is given in

333 Table ***3***.

334

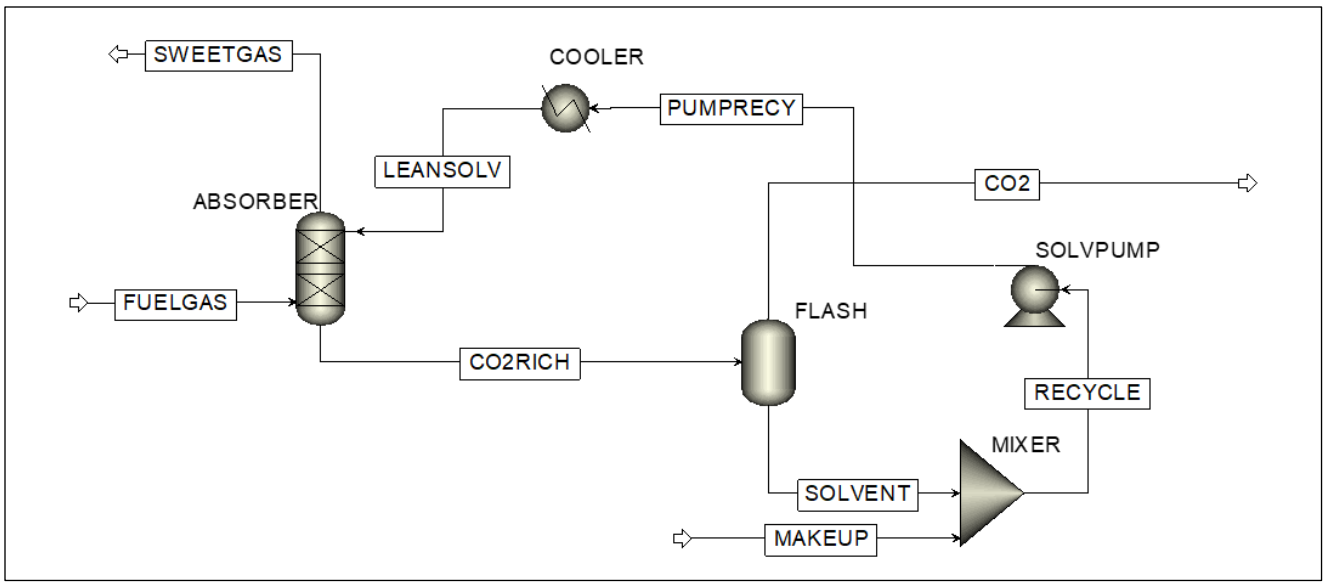

335

336 ***Figure 2. Process flow sheet of the solvent absorption pilot plant simulation***

337

338

Table 3. Summary of fixed conditions for trial #2 and input for process simulations.

Parameter	PEGDME	CASSH-1
Solvent temperature, °C	25	25
Solvent flow rate, $L \cdot h^{-1}$	32.0	32.4
Absorber column pressure, MPa	4.86	4.86
Syngas flow rate, $mol \cdot h^{-1}$	145.3	149.6
Syngas temperature, °C	37.8	37.3
L/G (Mass ratio inlet liq/gas)	6.9	6.5
Syngas composition (dry), mol%		
H_2	15.3	16.64
N_2	27.0	25.93
CO	1.06	0.71
CO_2	54.5	54.9
CH_4	1.77	1.41
H_2S	0.34	0.41
Flash temperature, °C	66	66
Flash pressure, MPa	0.1	0.1
Packed bed height, m	3.2	3.2
Absorber diameter, m	0.0762	0.0762
Absorber packing material	5/8 ” IMTP15	5/8 ” IMTP15

3 Results

3.1 Bench-Scale VLE Results

Measurement of VLE data of multicomponent systems is important for understanding and modeling the performance of physical solvent absorption processes. For the physical solvents tested in this study (PEGDME, CASSH-1, PEG-PDMS-3 and TBP) the solubility of CO_2 in the dry solvents increased with increasing pressure but decreased with increasing temperature, as shown in Figure 3. These trends are consistent with CO_2 solubility measured in other physical solvents. Dry PEGDME showed relatively higher CO_2 solubility compared to the hydrophobic solvents. To summarize and aid comparison of the solvents' performance, the solubility of CO_2 in each solvent at four temperatures and a CO_2 partial pressure of 1 MPa is shown in Table 4.

PEGDME shows slightly higher CO_2 solubility at 10 and 25°C, however, as the solvent temperature increases, the CO_2 solubility in PEGDME decreases at a faster rate than the hydrophobic solvents.

The solubility of other syngas components in the tested solvents showed that, at the same partial pressure, CH_4 was less soluble than CO_2 but more soluble than N_2 and H_2, as shown in Figure 4. For the hydrophobic solvents, the least soluble gases were H_2 followed by N_2, and the absorption performance of these gas components was less impacted by temperature compared to CO_2. Temperature dependent VLE data for N_2, H_2 and CH_4 can be found in the supplemental information. Experimental gas solubility for H_2, N_2 and CH_4 at 25°C and 1 MPa are shown in Table 5. The measured solubilities from the current study agree remarkably well with the computational predictions for CASSH-1 by Shi et al. (2021) who reported at 25°C and 0.1 MPa partial pressure a CO_2 solubility of 1.46 $mol \cdot L^{-1} \cdot MPa^{-1}$, H_2 solubility of 0.0220 $mol \cdot L^{-1} \cdot MPa^{-1}$, N_2 solubility of 0.0389 $mol \cdot L^{-1} \cdot MPa^{-1}$ and CH_4 solubility of 0.210 $mol \cdot L^{-1} \cdot MPa^{-1}$. As shown in Table 6, the highest gas pair selectivity for all solvents was CO_2/H_2, when compared to N_2 and CH_4, while CO_2/H_2 selectivity was highest for PEGDME followed by CASSH-1, PEG-PDMS-3 and then TBP.. Furthermore, the experimental solubility selectivity values agreed reasonably well with the computational predictions for CASSH-1 from Shi et al. (2021) who at 25°C reported CO_2/H_2 selectivity of 66.4, CO_2/N_2 selectivity of 37.6 and CO_2/CH_4 selectivity of 6.96.

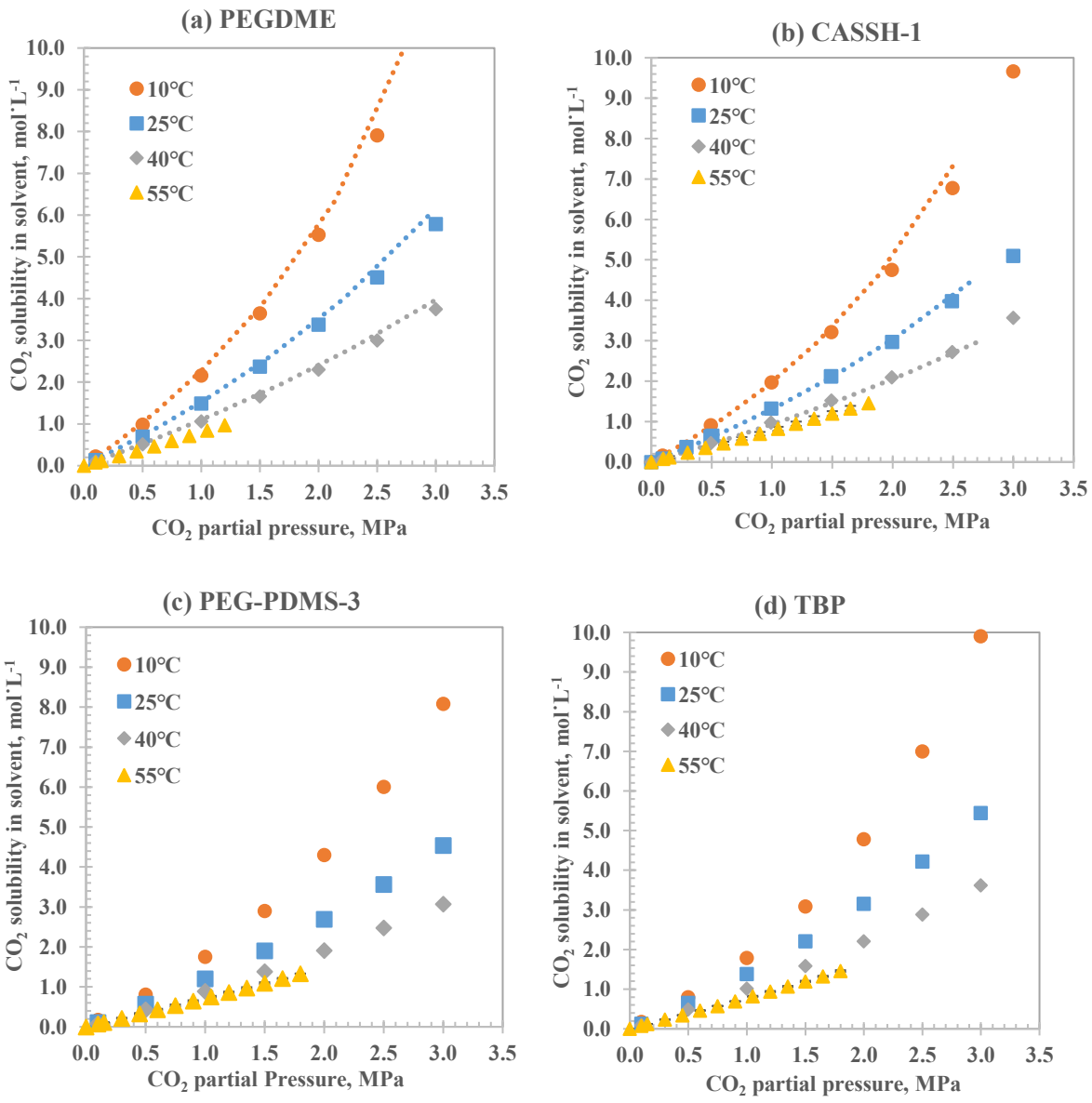

Figure 3: Experimental equilibrium CO_2 solubility as a function of its partial pressure at different temperatures in dry physical solvents (a) PEGDME, (b) CASSH-1, (c) PEG-PDMS-3, (d) TBP. These data were measured using the bench scale Isorsorp VLE apparatus for 10, 25 and 40°C. Data at 55°C was measured using the bench scale Hiden IGA VLE apparatus. Statistical error is represented by error bars (standard deviation, CI=68%) from 4 repeated measurements and the error is within the data point labels in most cases. Raw data can be found in the Supplemental Information. PC-SAFT EOS predictions have been included for PEGDME and CASSH-1 at 10, 25 and 40°C (shown as dashed lines).

Table 4. Experimental equilibrium CO_2 solubility as a function of temperature in dry PEGDME, CASSH-1, PEG-PDMS-3 and TBP. These data were measured using the bench-scale IGA VLE apparatus. Results are presented for a CO_2 partial pressure of 1 MPa. The statistical error is calculated as the standard deviation from 4 repeated measurements.

Temperature	**CO_2 solubility at 1 MPa (mol×L^{-1})**			
	PEGDME	**CASSH-1**	**PEG-PDMS-3**	**TBP**
10°C	2.26 ± 0.02	1.88 ± 0.019	1.82 ± 0.007	1.97 ± 0.010
25°C	1.50 ± 0.01	1.34 ± 0.009	1.25 ± 0.004	1.37 ± 0.007
40°C	1.10 ± 0.01	1.01 ± 0.003	0.906 ± 0.002	1.03 ± 0.002
55°C	0.80 ± 0.01	0.78 ± 0.002	0.718 ± 0.002	0.78 ± 0.001

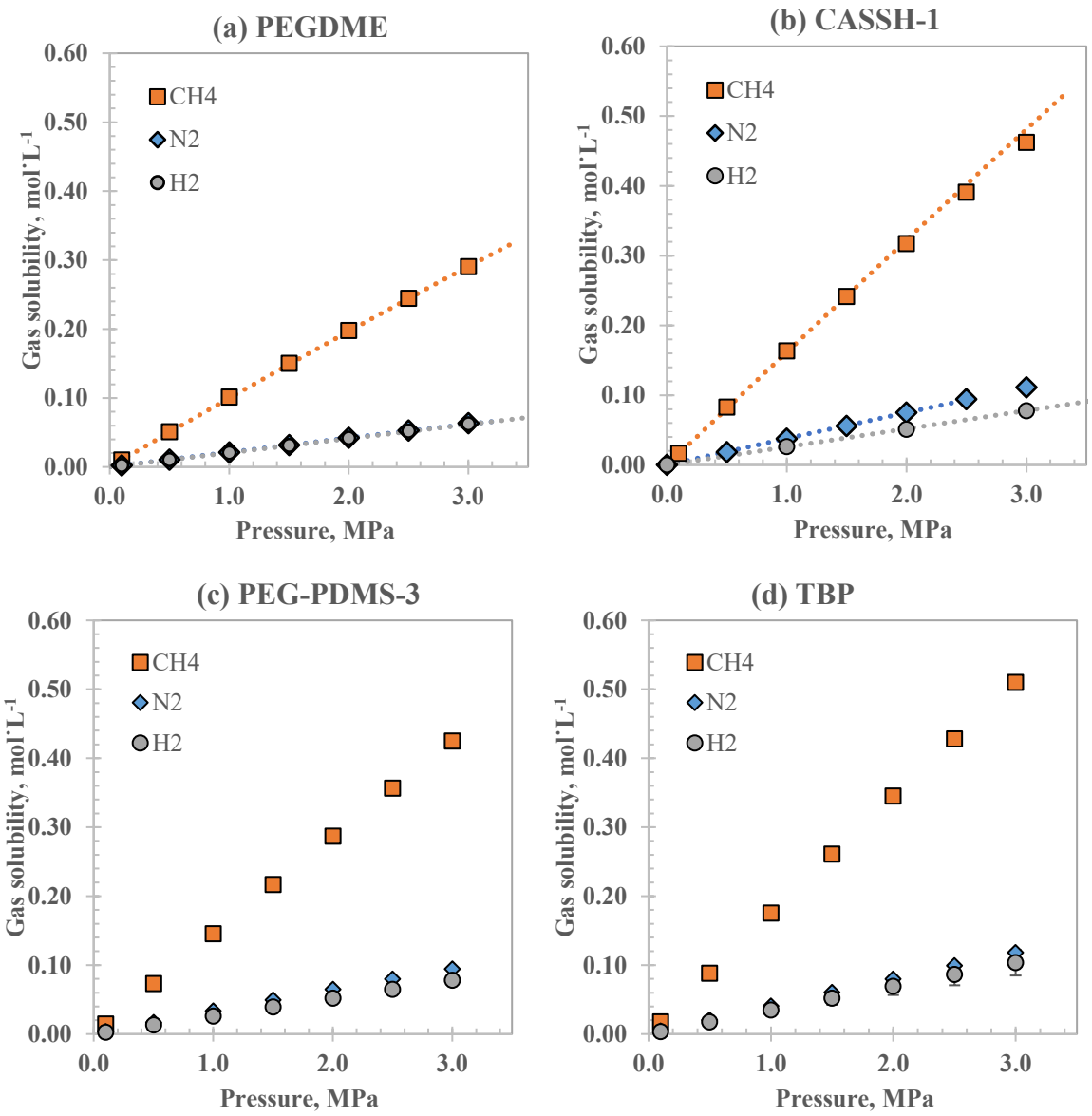

Figure 4. Equilibrium pure gas solubility at 25°C for CH_4, N_2 and H_2 as a function of pressure in dry physical solvents (a) PEGDME, (b) CASSH-1, (c) PEG-PDMS-3 (d) TBP. These data were measured using the Isosorp VLE apparatus. Statistical error is represented by error bars (standard deviation, CI=68%) from repeated measurements and the error is within the data point labels in most cases. Raw data can be found in the Supplemental Information. PC-SAFT EOS predictions have been included for PEGDME and CASSH-1 (shown as dashed lines).

Table 5. Equilibrium gas solubility in dry PEGDME, CASSH-1, PEG-PDMS-3 and TBP at gas partial pressure of 1 MPa and temperature of 25 °C. CO_2 solubility was measured using the IGA VLE apparatus and H_2, N_2 and CH_4 solubilities were measured using the Isosorp VLE apparatus. The statistical error for gas solubility is represented as the standard deviation from 4 repeated measurements.

Gas	Gas solubility at 25 °C & 1 MPa ($mol \cdot L^{-1}$)			
	PEGDME	**CASSH-1**	**PEG-PDMS-3**	**TBP**
H_2	0.021 ± 0.001	0.026 ± 0.002	0.026 ± 0.002	0.035 ± 0.003
N_2	0.021 ± 0.0003	0.037 ± 0.002	0.033 ± 0.003	0.04 ± 0.0008
CH_4	0.10 ± 0.001	0.16 ± 0.004	0.15 ± 0.005	0.18 ± 0.003
CO_2	1.50 ± 0.019	1.34 ± 0.020	1.25 ± 0.007	1.37 ± 0.013

Table 6. Equilibrium pure gas selectivity of CO_2 over H_2, N_2 and CH_4 at 25°C and 1 MPa gas partial pressure in dry PEGDME, CASSH-1, PEG-PDMS-3 and TBP. CO_2 solubility was measured using the IGA VLE apparatus and H_2, N_2 and CH_4 was measured using the Isosorp VLE apparatus.

Solvent	**PEGDME**	**CASSH-1**	**PEG-PDMS-3**	**TBP**
CO_2/H_2 Selectivity	71 ± 4	52 ± 4	48 ± 4	39 ± 3
CO_2/N_2 Selectivity	71 ± 1	36 ± 2	38 ± 3	34 ± 1
CO_2/CH_4 Selectivity	15 ± 0.2	8 ± 0.2	8 ± 0.3	8 ± 0.1

Given the favorable physical properties of these hydrophobic physical solvents (e.g. low viscosity, low vapor pressure, low water absorption, etc.) and comparable gas solubility results compared to the hydrophilic solvent (PEGDME) baseline, it was decided to further screen all four solvents in trial #1 of pre-combustion pilot plant testing.

3.2 Pilot Plant Trial 1 – Solvent Screening Results

The goal of the pilot plant trial #1 was to develop a performance baseline for the commonly studied physical solvent PEGDME (Selexol surrogate) and then compare its performance to the three hydrophobic physical solvents using the same pilot plant at comparable operating conditions. All four solvents (PEGDME, CASSH-1, PEG-PDMS-3 and TBP) were operated successfully in the pilot plant at similar operating conditions, with CO_2 absorption performance shown in

Table 7 which were obtained using syngas with properties shown in Table 2 and at solvent flow rates of between 37 and 45 $L \cdot h^{-1}$. When operating with an L/G ratio of ~8, all four solvents achieved greater than 97% CO_2 removal and 96% H_2S removal. Compared to the performance of PEGDME at the recommended Selexol process operating temperature of 10°C, the hydrophobic solvents CASSH-1, PEG-PDMS-3 and TBP all showed comparable or higher CO_2 and H_2S absorption performance, including at elevated solvent inlet temperatures of up to 40°C. PEGDME was not tested at 55 °C since the Selexol absorption process is typically operated at no more than ~38 °C (100 °F) (Cowan et al., 2011).

Table 7. Pilot plant trial #1 solvent absorption performance results in PEGDME, CASSH-1, PEG-PDMS-3 and TBP at solvent flow rates of ~37-45 L/hr. CO_2 partial pressure in the syngas was ~2.6 MPa and H_2S partial pressure in the syngas was ~0.023 MPa. For gas uptake, the first listed error is the statistical error from repeated measurements represented as the standard deviation (CI=68%), and the second error is the systematic error from calibration uncertainty in gas/liquid flow meters.

Solvent Temperature*	Performance parameter	PEGDME	CASSH-1	PEG-PDMS-3	TBP
10°C	Solvent temperature inlet / outlet, °C	10.1 / 13.8	10.4 / 28.5	9.5 / 20.5	10.7 / 13.9
	CO_2 gas uptake, mol×L^{-1}	1.64 ± 0.10 ± 0.10	2.27 ± 0.03 ± 0.14	1.72 ± 0.10 ± 0.10	1.50 ± 0.06 ± 0.09
	H_2S gas uptake, mol×L^{-1}	0.014 ± 0.001 ± 0.001	0.021 ± 0.001 ± 0.001	0.014 ± 0.001 ±0.001	0.015 ± 0.001 ± 0.001
25°C	Solvent temperature inlet / outlet, °C	25.0 / 27.0	25.6 / 32.6	25.3 / 33.6	25.1 / 26.8
	CO_2 gas uptake, mol×L^{-1}	1.46 ± 0.14 ± 0.09	1.66 ± 0.04 ± 0.10	1.63 ± 0.02 ± 0.10	1.65 ± 0.04 ± 0.10
	H_2S gas uptake, mol×L^{-1}	0.011 ± 0.001 ± 0.001	0.015 ± 0.001 ± 0.001	0.012 ± 0.001 ± 0.001	0.016 ± 0.001 ± 0.001
40°C	Solvent temperature inlet / outlet, °C	**	40.6 / 48.0	40.0 / 46.6	39.8 / 41.4
	CO_2 gas uptake, mol×L^{-1}	**	1.91 ± 0.05 ± 0.11	1.64 ± 0.07 ± 0.10	1.90 ± 0.01 ± 0.11
	H_2S gas uptake, mol×L^{-1}	**	0.018 ± 0.001 ± 0.001	0.014 ± 0.001 ± 0.001	0.018 ± 0.001 ± 0.001
55°C	Solvent temperature inlet / outlet, °C	**	55.4 / 57.4	54.3 / 63.7	55.5 / 58.5
	CO_2 gas uptake, mol×L^{-1}	**	1.67 ± 0.05 ± 0.10	1.55 ± 0.10 ± 0.09	1.92 ± 0.01 ± 0.12
	H_2S gas uptake, mol×L^{-1}	**	0.016 ± 0.001 ± 0.001	0.014 ± 0.001 ± 0.001	0.018 ± 0.001 ± 0.001
Water content of solvent at end of trial, ppm		4000**	550	1550	1670

* An absorber temperature range is provided for each nominal solvent temperature. The lower temperature is the absorber inlet solvent temperature (solvent enters at the top of the absorption column), and the higher temperature is the solvent temperature at the bottom of the absorption column. As the syngas enters at approximately 38°C and the absorption process is exothermic, there is a temperature gradient from the top to bottom of the column.

**PEGDME solvent testing was not conducted at the highest solvent inlet temperature of 55°C and data were not included if mass balance errors were greater than 20% (which was the case for data collected with PEGDME at 40°C).

The performance results obtained from this screening study provided confidence in using hydrophobic physical solvents as an alternative to traditional hydrophilic physical solvents like Selexol for pre-combustion CO_2 capture, particularly when comparing absorption performance at higher temperatures. The most promising hydrophobic solvent performance was provided by CASSH-1 as indicated by high CO_2 solubility and the lowest water miscibility at ambient temperatures. CASSH-1 has been reported in previous laboratory and simulation-based studies to be a low-cost hydrophobic physical solvent for CO_2 absorption while maintaining low viscosity, low vapor pressure, low corrosion potential, and low foaming tendency (Shi et al., 2021; Siefert and Hopkinson, 2018). These characteristics along with the results from this pilot plant solvent screening study led to the selection of CASSH-1 and PEGDME (for baseline performance comparison) for longer term pilot plant testing using syngas from the coal based IGCC pilot plant.

3.3 Pilot Plant Trial 2 – Long Term Solvent Performance Results (PEGDME and CASSH-1)

The goal of pilot plant trial #2 was to assess both PEGDME (baseline hydrophilic solvent, i.e., Selexol surrogate) and CASSH-1 (NETL's hydrophobic solvent) for any changes in plant performance or solvent properties over a longer period of time while using coal-derived syngas. The collected data were also used to compare pilot plant performance against process simulations developed using equilibrium VLE data for pure gas components (CO_2, CH_4, N_2, H_2). Syngas can contain a range of trace components, including mercury, hydrogen selenide, arsine, carbonyls, and organic tars, that over time could accumulate in the process and could impact the solvent properties and overall absorption performance. During Trial 2 the syngas had relatively constant levels of H_2, CO, N_2 CO_2 and CH_4, although there was a slight but steady decrease in H_2S concentration when PEGDME was used. The gas composition trends for the 10 days of pilot plant operation (Days 1-5 for CASSH-1 and Days 6-10 for PEGDME) for the syngas, sweet gas, and acid gas are shown in Figure 5.

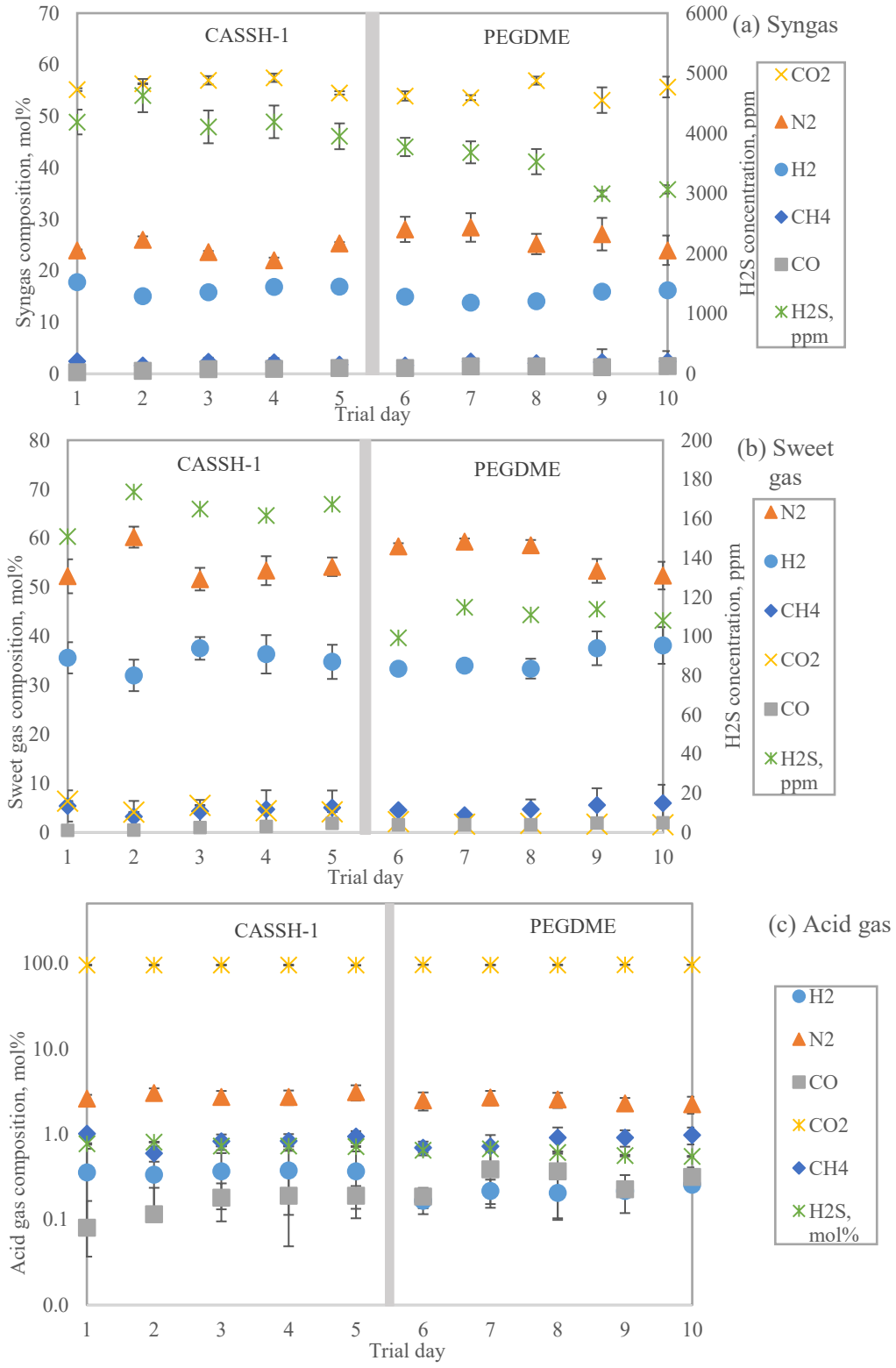

Figure 5. Gas composition (dry) measured for (a) syngas, (b) sweet gas and (c) acid gas for each day of Trial # 2 (Days 1-5: CASSH-1; Days 6-10: PEGDME). These normalized gas composition

values represent averages from the two gas analyzers on each gas stream and error bars are represented by the standard deviation (CI=68%, statistical error only).

Both solvents were operated with a solvent flow rate of approximately 32 $L \cdot h^{-1}$ (32.0 ± 0.4 $L \cdot h^{-1}$ for PEGDME and 32.4 ± 0.4 $L \cdot h^{-1}$ for CASSH-1), solvent inlet temperature of approximately 25°C (25.0°C for PEGDME and 24.5°C for CASSH-1) and gas inlet temperature of approximately 37°C (37.8°C for PEGDME and 37.3°C for CASSH-1). The dry gas composition data were used to compare the absorption performance of each solvent using equation (4) for normalized gas uptake. Error bars were calculated based on the standard deviation provided from 5 days of operation plus spot checks for each solvent using gas composition data from two different gas analyzers. Two methods for determining gas uptake into the solvent were also averaged for these calculations - (1) the difference between CO_2 entering and exiting the absorber and (2) the amount of CO_2 removed from the solvent flash/regeneration process. At an L/G ratio of ~7, both solvents achieved greater than 97% CO_2 removal and 98% H_2S removal. Water absorption into the solvents was measured at the end of each 5-day testing period. CASSH-1 contained 358 ppm water, which was less than half that of PEGDME which still contained 837 ppm water after the flash process. Although the hydrophobic solvent CASSH-1 contained less water than the hydrophilic solvent PEGDME, it should be highlighted that this was measured after the solvent flash process which would have removed most of the absorbed water with the CO_2. PEGDME, a hydrophilic solvent, will absorb large amounts of water from feed gas streams which will then impair CO_2 loading capacity (Samipour et al., 2020). The absorption performance results in terms of gas uptake for PEGDME and CASSH-1 after 5 continuous days of operation for each solvent are shown in Table 8.

Table 8. Inlet syngas partial pressure (MPa) and gas uptake ($mol \cdot L^{-1}$) into PEGDME and CASSH-1 over 5 days of continuous plant operation in Trial 2. Solvent inlet temperature: 25°C, Solvent outlet temperature: 36°C (PEGDME) & 40°C (CASSH-1). PEGDME: Inlet solvent flow rate: 32.0±1.9 $L \cdot h^{-1}$, Inlet syngas temperature: 37.8°C, Syngas flow rate: 145±1 $mol \cdot hr^{-1}$. CASSH-1: Inlet solvent flow rate: 32.4±1.9 $L \cdot h^{-1}$, Inlet syngas temperature: 37.3°C, Syngas flow rate: 150 ±4 $mol \cdot hr^{-1}$. For partial pressure, the "±" value is the statistical standard deviation (CI=68%) from the inlet gas composition measurements. For the gas uptake, the first standard deviation (CI=68%) is statistical from gas analyzers, and the second standard

deviation (CI=68%) is <u>systematic</u> from calibration uncertainty in gas/liquid flow meters, which would cancel out in estimates of ratios, such as the ratio of CO_2 to H_2 uptake, which is not listed below due to the different inlet syngas partial pressures and due to non-equilibrium conditions in the absorber.

Gas component	Syngas partial pressure, MPa		Gas uptake, mol·L^{-1}	
	PEGDME	**CASSH-1**	**PEGDME**	**CASSH-1**
CO_2	2.65 ± 0.07	2.67 ± 0.05	2.49 ± 0.06 ± 0.15	2.40 ± 0.13 ± 0.14
N_2	1.31 ± 0.10	1.26 ± 0.05	0.070 ± 0.005 ± 0.004	0.073 ± 0.008 ± 0.004
H_2	0.74 ± 0.02	0.81 ± 0.01	0.0070 ± 0.0005 ± 0.0004	0.011 ± 0.004 ± 0.001
CH_4	0.09 ± 0.02	0.07 ± 0.01	0.020 ± 0.005 ± 0.001	0.020 ± 0.005 ± 0.001
CO	0.05 ± 0.02	0.034 ± 0.005	0.0070 ± 0.0007 ± 0.0004	0.0040 ± 0.0007 ±0.0003
H_2S	0.017 ± 0.001	0.020 ± 0.001	0.0156 ± 0.0004 ± 0.0010	0.0186 ± 0.0003 ± 0.0011

3.4 Process Simulation Results and Comparison to Pilot Plant Data

Process simulations were developed for Trial 2 of the UND EERC pilot plant operation with the solvents PEGDME and CASSH-1. Binary interaction parameters, that were regressed from the experimentally measured VLE data presented in section 3.1, were used with the PC-SAFT EOS property model to predict absorption performance. Details on the binary interaction parameters can be found in the Supplemental Information Table S8. Rate-based and equilibrium models were applied. The equilibrium model assumes the vapor and liquid phases leaving each stage are in thermodynamic equilibrium while the rate-based model assumes that mechanical, chemical and thermodynamic equilibrium occur at the gas-liquid interface and mass transfer is described by the two-film theory (Afkhamipour and Mofarahi, 2013; Borhani et al., 2015; Ma et al., 2018). The

rate-based model incorporates the mass transfer rate via correlations for mass transfer coefficients, gas-liquid interfacial area and diffusion coefficients which consider solvent physical properties such as density, viscosity, and surface tension. Results from the simulations are compared to the measured pilot plant data in Table 9 which shows both the rate based model and the equilibrium model were able to predict the performance of the pilot plant with reasonable accuracy given inherent errors associated with pilot plant operation and measurement of gas composition. The rate-based model provided slightly better predictions than the equilibrium model for CASSH-1 while both the rate-based and equilibrium models were similar for PEGDME which is likely due to the system operating close to equilibrium conditions as a result of high solvent flow rates. To assess the impact of solvent flow rate, the rate-based simulation was operated with solvent flow rates ±1 standard deviation of the average flow rate with results provided in Table S9 of the Supplemental Information. Increasing the solvent flow rate resulted in higher CO_2 removal efficiency while decreasing solvent flow rate reduced CO_2 removal efficiency and both models were able to predict plant performance within expected error. The prediction of temperature profile was generally within experimental error with lower solvent flow rate resulting in higher predictions for temperature profile in the absorber. It should be noted that the temperature measured in the pilot plant was likely impacted by heat losses to the surroundings which were not accounted for in the simulation.

Table 9. Pilot plant output data from trial #2 for PEGDME and CASSH-1 compared to Aspen Plus process simulation predictions. The input operating conditions for the simulation can be found in Table 3 ***and the process flow sheet can be found in Figure 2.***

Solvent:	**PEGDME**			**CASSH-1**		
Property	**Pilot plant**	**Equilibrium model Prediction**	**Rate-based model Prediction**	**Pilot plant**	**Equilibrium model Prediction**	**Rate-based model Prediction**
Absorber temperature profile						
Top of column	24.9 ± 0.3	24.8	25.4	28.7 ± 1.3	24.4	24.9
Upper	25.5 ± 0.7	24.8	26.5	34.0 ± 1.5	24.8	26.1
Mid	26.7 ± 1.6	25.3	28.3	37.7 ± 1.1	26.5	28.0
Lower	30.1 ± 2.8	28.1	31.1	39.6 ± 0.7	31.0	30.9
Bottom of column	36.4 ± 2.0	35.3	35.0	40.0 ± 0.6	35.8	34.3
Sweet gas flow rate, mol/h	59.3 ± 1.0	62.9	68.1	67.1 ± 5.2	63.4	68.2
Sweet gas, mol%						
H_2	36.5 ± 1.0	33.8	31.3	35.0 ± 2.1	37.4	34.7
N_2	55.4 ± 1.0	59.4	55.0	54.6 ± 1.5	57.1	52.9
CO	1.73 ± 0.04	2.1	1.9	1.1 ± 0.1	1.6	1.4
CO_2	1.6 ± 0.2	1.2	8.6	5.1 ± 0.3	1.4	8.6
CH_4	4.9 ± 0.1	3.4	3.2	4.2 ± 0.3	2.6	2.4
H_2S	0.012 ± 0.001	0.006	0.006	0.017 ± 0.001	0.009	0.009
Acid gas flow rate, mol/h	85.0 ± 1.0	82.4	77.2	81.3 ± 3.3	86.2	81.4
Acid gas, mol%						
H_2	0.21 ± 0.04	1.2	1.2	0.45 ± 0.15	1.4	1.5
N_2	2.6 ± 0.2	2.1	2.2	3.2 ± 0.40	3.0	3.3
CO	0.25 ± 0.05	0.3	0.3	0.14 ± 0.10	0.08	0.09
CO_2	95.6 ± 0.2	95.3	95.1	94.6 ± 0.30	94.3	93.8
CH_4	0.78 ± 0.10	0.52	0.54	0.82 ± 0.08	0.56	0.62
H_2S	0.60 ± 0.05	0.60	0.64	0.74 ± 0.01	0.71	0.75
CO_2 recovery, %	99.0 ± 0.5	99	93	95 ± 5	99	93
CO_2 uptake, mol·L^{-1}·	**2.49±0.06±0.15**	**2.46**	**2.30**	**2.40±0.13±0.14**	**2.52**	**2.37**
Calculations for experimental mole balance check						
Inlet gas flow rate, mol/h	145±1			150±4		
Molar ratio of outlets to inlet	99.5%±1.2%			99%±5%		

4 Discussion

During Trial #1, all four solvents achieved >97% CO_2 removal and >96% H_2S removal. It should be noted that the solvent regeneration process at UND EERC was not intended to reflect optimal regeneration performance. Typically, solvent regeneration is conducted using at least three stages of regeneration, the first of which includes recycle back to the syngas to minimize H_2 loss in the acid gas. Also, higher solvent regeneration temperatures using low grade waste heat from the power plant could be used to increase recovery rates and decrease the energy requirements of acid gas capture. This would result in lower operating costs for solvent regeneration and produce a CO_2 gas stream at higher pressure which minimizes compression costs that would be required for sequestration. During Trial #2, at a constant solvent flow rate, the flash tank solvent temperature was increased from 43°C to 66°C. This increase in solvent regeneration temperature appears to have improved H_2 recovery for both PEGDME and CASSH-1, and increased the CO_2 uptake for both solvents by 20-30% when operated at a solvent temperature of 25°C. However, although the higher regeneration temperature appeared to improve the absorption performance for PEGDME, it also resulted in significant losses of PEGDME solvent as a result of the higher vapor pressure of PEGDME. This was observed experimentally via the knockout pot on the CO_2 stream exiting the flash drum which contained approximately twice as much PEGDME solvent compared to CASSH-1 solvent. The costs of reclaiming this PEGDME solvent would need to be balanced with the benefit of higher CO_2 uptake at these elevated temperatures. During Trial #2, the CO_2 absorption performance of CASSH-1 may have been impacted by competing H_2S absorption due to the slightly higher H_2S concentration in the syngas during the first 5 days of operation with CASSH-

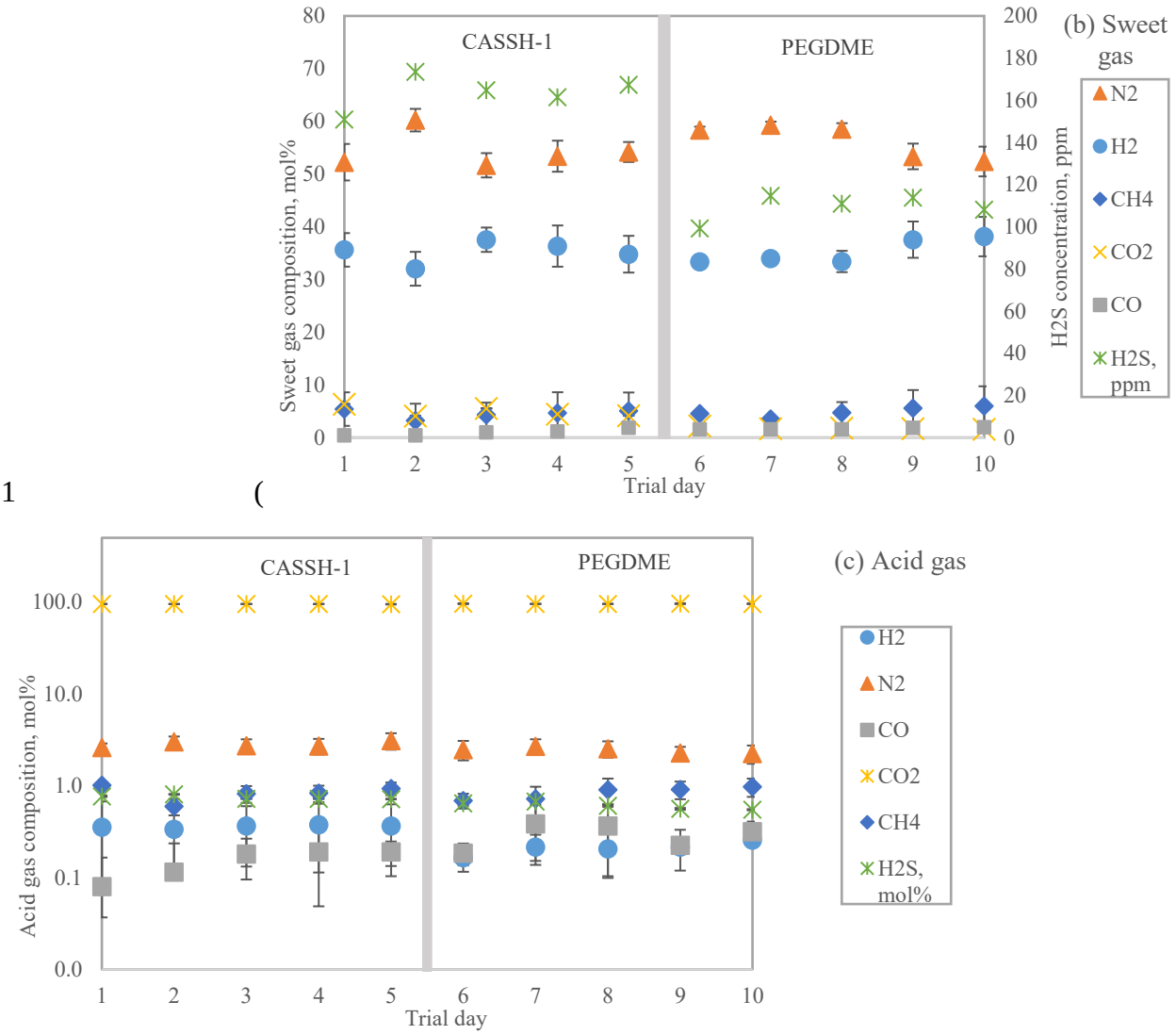

564 1 (

565

566 ***Figure 5. Gas composition (dry) measured for (a) syngas, (b) sweet gas and (c) acid gas for each***
567 ***day of Trial # 2 (Days 1-5: CASSH-1; Days 6-10: PEGDME). These normalized gas composition***
568 ***values represent averages from the two gas analyzers on each gas stream and error bars are***
569 ***represented by the standard deviation (CI=68%, statistical error only).***

570). Both PEGDME and CASSH-1 solvents will absorb CO_2 as well as H_2S and both solvents showed
571 comparable H_2S removal performance of approximately 98%.

572 Several solvent temperatures were assessed in the first set of pilot plant trials. At the
573 recommended Selexol process operating temperature of 10 °C, all of the hydrophobic solvents
574 showed comparable or higher CO_2 and H_2S absorption performance compared to PEGDME, while

575 the hydrophobic solvents continued to have high gas absorption at inlet temperatures of up to 55
576 °C (

Table 7). Operation at higher absorption temperatures is expected to reduce the energy and capital costs associated with the costly and energy intensive refrigeration equipment that is required to operate hydrophilic physical solvents, such as methanol and PEGDME, in their currently designed commercial processes. During Trial #2 when both PEGDME and CASSH-1 were operated continuously at 25°C with CO_2 partial pressure of ~ 2.7 MPa both solvents showed comparable absorption performance in terms of the CO_2 uptake (2.49 and 2.40 $mol \cdot L^{-1}$ for PEGDME and CASSH-1, respectively) and uptake of other syngas components (Table 8). These results were lower than that predicted from the pure gas equilibrium measurements reported in this study and in the literature by Shi et al. ((Shi et al., 2019; Shi et al., 2021) but this is to be expected when operating with a multi component syngas in an absorption column setup.

Hydrophobic physical solvents are expected to absorb less water, which is ideal in the case of pre-combustion CO_2 capture. Low water solubility is an important property for pre-combustion solvent absorption applications as it keeps the water in the sweet gas with the H_2 which can increase power output from the gas turbine and reduces the need for costly water recovery equipment. Additionally, water in the solvent can lead to equipment corrosion and reduced CO_2 absorption capacity due to the reduced mass transfer rates as a result of increased solvent viscosity and competition from the water molecules which could form stronger bonds with the solvent compared to CO_2. Lower residual water solubility (after the flash process) was observed in both pilot plant trials with the hydrophobic solvents. Process simulations also indicated that hydrophilic PEGDME would contain approximately twice as much water as hydrophobic CASSH-1 before the flash process and more than three times as much water after the flash process (Process simulation results can be found in the Supplemental Information). PEGDME contained significantly more water than the three hydrophobic solvents in Trial #1 (Table 7) and although CASSH-1 and PEGDME showed similar CO_2 absorption performance by the end of Trial #2, the hydrophobic solvent CASSH-1 contained less than half (358 ppm) the amount of water than PEGDME (837 ppm) which was measured after the solvent regeneration process where most water is flashed out of the solvent with the CO_2. The measured water content in both solvents during the second trial was lower than the first trial which was likely impacted by the higher flash temperature in the second trial. As shown in the VLE measurements presented in Figure 3 and Table 4, CO_2 uptake in dry PEGDME is higher than that in dry CASSH-1, however, in the pilot plant trials both solvents

have similar CO_2 absorption performance which is most likely due to reduced CO_2 capacity of the wet hydrophilic PEGDME solvent.

Gas absorption selectivity was calculated to assess how the solvent absorbs CO_2 compared to the other gas components present in the syngas. Ideally, the solvent will absorb CO_2 (and potentially H_2S) while rejecting the other syngas components, particularly H_2. CO_2 selectivity over H_2 was high (~60) for all solvents in Trial #1. During Trial #2 the CO_2/H_2 selectivity was 66 ± 6 for CASSH-1 and 99 ± 8 for PEGDME. The trends for gas electivity between CASSH-1 and PEGDME measured using VLE equipment (Table 6) and the pilot plant were similar with CO_2/H_2 > CO_2/N_2 > CO_2/CO > CO_2/CH_4 > CO_2/H_2S.

Another important outcome from operation of this pilot plant was assessing the solvent interactions with other minor components present in the syngas. In general, the solvents used in this study did not show signs of solvent degradation after operation with coal-derived syngas, as indicated by consistent CO_2 absorption performance over the testing period. During Trial #2, Dräger tubes were used with the solvents to assess the presence of minor syngas components such as HCN, NH_3, HCl, benzene, toluene and xylene. The pilot plant contained a quench pot system upstream of the solvent absorption, which appears to have removed most of the tars and water-soluble contaminants, such as NH_3 and HCl. The main components that were detected in the solvents were HCN and toluene. Semi-quantitative analysis was used to identify absorption of tar compounds and both solvents were found to absorb similar amounts of aromatic compounds, like toluene and benzene. However, CASSH-1 was found to have absorbed more polycyclic tar compounds, like naphthalene compared to PEGDME, although the total amount of tar materials in both solvents was relatively low. The presence of these contaminants did not appear to impact solvent performance, although further testing is recommended to quantify these components and their impact with more accuracy.

All four physical solvents were operated close to equilibrium conditions in the pilot plant trials, however ideal operation is not expected due to variations in solvent physical properties (e.g., change in viscosity due to water absorption), temperature variations and/or due to competitive absorption of other syngas components. The syngas was a mixed gas stream with multiple gas components, including sulfur, tars, and water, which impacted the absorption performance. Both rate-based and equilibrium models were used in process simulations to model the pilot plant. Both models were able to predict plant performance with reasonable accuracy; however, in general the

638 rate-based model is preferred over the equilibrium model due to the inclusion of parameters that
639 better describe column hydrodynamics and mass transfer and therefore is able to better represent
640 the actual absorption column performance. The rate-based model includes rates of multi-
641 component mass and heat transfer directly with the mass transfer described via the two-film theory
642 (Noeres et al., 2003), which incorporates mass transfer coefficient correlations that are dependent
643 on physical properties and hydrodynamics and overall provide better representation of the actual
644 absorption column performance.
645
646 **5 Conclusions**
647 Equilibrium gas solubility data for the syngas components CO_2, H_2, N_2 and CH_4 were measured
648 for the baseline PEGDME hydrophilic solvent and the novel hydrophobic physical solvents
649 (CASSH-1, PEG-PDMS-3 and TBP) over a range of pressures and temperatures relevant to pre-
650 combustion CO_2 capture. The solubility of CO_2 in all solvents increased with increasing pressure
651 but decreased with increasing temperature. The hydrophobic physical solvents, which have more
652 favorable physical properties compared to PEGDME (e.g., lower viscosity, lower vapor pressure,
653 lower water uptake, etc.) also showed comparable gas solubility results compared to the
654 hydrophilic solvent baseline. Therefore, it was decided to further screen the performance of all
655 four solvents in a pre-combustion pilot plant using coal derived syngas.
656 Operating experience and operational data were obtained for benchmarking the three
657 hydrophobic solvents including CASSH-1, PEG-PDMS-3 and TBP, against the commercial
658 hydrophilic solvent PEGDME. All four solvents were operated successfully in the pilot plant at
659 similar operating conditions and showed comparable CO_2 absorption performance. However,
660 compared to the performance of PEGDME at the recommended Selexol process operating
661 temperature of 10°C, the hydrophobic solvents all showed comparable or higher CO_2 uptake
662 performance at elevated temperatures of up to 55°C. Additionally, the hydrophobic solvents
663 absorbed less water from the syngas, particularly CASSH-1, compared to PEGDME. Longer term
664 solvent testing was subsequently completed for the hydrophilic solvent PEGDME and the
665 hydrophobic solvent CASSH-1. The results showed that both solvents absorbed CO_2 without any
666 significant degradation over the testing period, and both showed comparable absorption
667 performance as indicated by similar CO_2 uptake and similar gas selectivity. However, despite some
668 minor absorption of syngas contaminants, the hydrophobic solvent CASSH-1 absorbed less water

and was capable of operation at higher absorption temperatures (up to 55°C) which makes it a promising option for use as a physical solvent for CO_2 removal from future gasification applications. Absorption of less water into the solvent will reduce solvent dehydration processing costs, reduce the loss of water from the syngas, and enable operation at higher temperatures to reduce the need for energy intensive cooling of the solvent. Further work is required to optimize and test solvent regeneration using a multi-stage flash process operated at higher temperatures and pressures which could decrease the need for costly re-compression of the CO_2 gas stream before sequestration.

Results from this study, including equilibrium data, pilot plant testing results and process simulations, will build confidence in the use of novel hydrophobic solvents for CO_2 capture from high pressure syngas. Operation of the pilot plant provided valuable operating data for validation of process simulations which is an important step for the design and scale-up of novel processes and will help encourage deployment of larger industrial applications. And finally, although the experimental program covered in this work is aimed at CO_2 capture from IGCC power generation, the hydrophobic physical solvents tested in this study are also applicable to other high pressure synthetic gas applications including adjustment of CO/H_2 ratio for coal-to-liquids and biomass-to-liquids, production of H_2 from reformed natural gas and removal of CO_2 from syngas used in other applications such as blue hydrogen or ammonia production.

6 Acknowledgements

This technical effort was performed in support of the US Department of Energy's Office of Fossil Energy & Carbon Management (FECM) Carbon Capture program. The research was executed through the NETL Research and Innovation Center's 2021 Transformational Carbon Capture field work proposal (FWP) and 2022 Point Source Capture FWP.

7 Disclaimer

privately owned rights. Reference herein to any specific commercial product, process, or service by trade name, trademark, manufacturer, or otherwise, does not necessarily constitute or imply its endorsement, recommendation, or favoring by the United States Government or any agency thereof. The views and opinions of authors expressed herein do not necessarily state or reflect those of the United States Government or any agency thereof.

8 References

Afkhamipour, M., Mofarahi, M., 2013. Comparison of rate-based and equilibrium-stage models of a packed column for post-combustion CO2 capture using 2-amino-2-methyl-1-propanol (AMP) solution. International Journal of Greenhouse Gas Control 15, 186-199.

Ashkanani, H.E., Wang, R., Shi, W., Siefert, N.S., Thompson, R.L., Smith, K., Steckel, J.A., Gamwo, I.K., Hopkinson, D., Resnik, K., Morsi, B.I., 2020. Levelized Cost of CO2 Captured Using Five Physical Solvents in Pre-combustion Applications. International Journal of Greenhouse Gas Control 101, 103135.

Billet, R., Schultes, M., 1993. A physical model for the prediction of liquid hold-up in two-phase countercurrent columns. Chemical Engineering & Technology 16, 370-375.

Borhani, T.N.G., Akbari, V., Afkhamipour, M., Hamid, M.K.A., Manan, Z.A., 2015. Comparison of equilibrium and non-equilibrium models of a tray column for post-combustion CO2 capture using DEA-promoted potassium carbonate solution. Chemical Engineering Science 122, 291-298.

Bucklin, R.W., Schendel, R.L., 1984. Comparison of Fluor solvent and Selexol processes. Energy progress 4, 137-142.

Cowan, R.M., Jensen, M.D., Pei, P., Steadman, E.N., Harju, J.A., 2011. Current status of CO2 capture technology development and application. Energy & Environmental Research Center, University of North Dakota, Grand Forks, ND.

Damen, K., Gnutek, R., Kaptein, J., Ryan Nannan, N., Oyarzun, B., Trapp, C., Colonna, P., van Dijk, E., Gross, J., Bardow, A., 2011. Developments in the pre-combustion CO2 capture pilot plant at the Buggenum IGCC. Energy Procedia 4, 1214-1221.

Enick, R.M., Koronaios, P., Stevenson, C., Warman, S., Morsi, B., Nulwala, H., Luebke, D., 2013. Hydrophobic Polymeric Solvents for the Selective Absorption of CO2 from Warm Gas Streams that also Contain H2 and H2O. Energy & Fuels 27, 6913-6920.

Franckwiak, S., Nitschke, E., 1970. Estasolva: new gas treating process. Hydrocarbon Process.; (United States), 145-148.

Global CCS Institute, 2021. Blue Hydrogen.

733 Kohl, A.L., Nielsen, R.B., 1997. Chapter 14 - Physical Solvents for Acid Gas Removal, in: Kohl,
734 A.L., Nielsen, R.B. (Eds.), Gas Purification (Fifth Edition). Gulf Professional Publishing,
735 Houston, pp. 1187-1237.

736 Koytsoumpa, E.I., Atsonios, K., Panopoulos, K.D., Karellas, S., Kakaras, E., Karl, J., 2015.
737 Modelling and assessment of acid gas removal processes in coal-derived SNG production.
738 Applied Thermal Engineering 74, 128-135.

739 Lau, H.C., Ramakrishna, S., Zhang, K., Radhamani, A.V., 2021. The role of carbon capture and
740 storage in the energy transition. Energy and Fuels 35, 7364-7386.

741 Leva, M., 1992. Reconsider packed-tower pressure-drop correlations. Chemical Engineering
742 Progress 88, 65-72.

743 Li, S., Jin, H., Mumford, K.A., Smith, K., Stevens, G., 2015. IGCC Precombustion CO2 Capture
744 Using K2CO3 Solvent and Utilizing the Intercooling Heat Recovered From CO2 Compressors
745 for CO2 Regeneration. Journal of Energy Resources Technology 137, 042002-042002.

746 Ma, C., Liu, C., Lu, X., Ji, X., 2018. Techno-economic analysis and performance comparison of
747 aqueous deep eutectic solvent and other physical absorbents for biogas upgrading. Applied
748 Energy 225, 437-447.

749 Moioli, S., Giuffrida, A., Gamba, S., Romano, M.C., Pellegrini, L., Lozza, G., 2014. Pre-
750 combustion CO2 capture by MDEA process in IGCC based on air-blown gasification. Energy
751 Procedia 63, 2045-2053.

752 Morton, F., Laird, R., Northington, J., 2013. The National Carbon Capture Center: Cost-effective
753 test bed for carbon capture R&D. Energy Procedia 37, 525-539.

754 Mumford, K.A., Wu, Y., Smith, K.H., Stevens, G.W., 2015. Review of solvent based carbon-
755 dioxide capture technologies. Frontiers of Chemical Science and Engineering 9, 125-141.

756 Nagar, A., McLaughlin, E., Hornbostel, M., Krishnan, G., Jayaweera, I., 2017. CO2 capture from
757 IGCC gas streams using the AC-ABC process, United States, p. Medium: ED; Size: 133 p.

758 Newman, S.H., 1985. Acid and Sour Gas Treating Processes. Gulf Publishing Co.,Houston, TX.

759 Noeres, C., Kenig, E.Y., Górak, A., 2003. Modelling of reactive separation processes: reactive
760 absorption and reactive distillation. Chemical Engineering and Processing: Process
761 Intensification 42, 157-178.

762 Onda, K., Takeuchi, H., Okumoto, Y., 1968. Mass transfer coefficients between gas and liquid
763 phases in packed columns. Journal of Chemical Engineering of Japan 1, 56-62.

764 Piché, S., Larachi, F., Grandjean, B.P.A., 2001. Flooding Capacity in Packed Towers: Database,
765 Correlations, and Analysis. Industrial & Engineering Chemistry Research 40, 476-487.

766 Samipour, S., Manshadi, M.D., Setoodeh, P., 2020. Chapter 20 - CO2 removal from biogas and
767 syngas, in: Rahimpour, M.R., Farsi, M., Makarem, M.A. (Eds.), Advances in Carbon Capture.
768 Woodhead Publishing, pp. 455-477.

769 Shi, W., Hopkinson, D.P., Steckel, J.A., Resnik, K., Macala, M.K., Thompson, R.L., Tiwari, S.,
770 2018. A Data Mining Method for the Identification of New Physical Solvents, 2018 NETL CO2
771 Capture Technology Project Review Meeting, Pittsburgh, USA.

772 Shi, W., Siefert, N.S., Baled, H.O., Steckel, J.A., Hopkinson, D.P., 2016. Molecular Simulations
773 of the Thermophysical Properties of Polyethylene Glycol Siloxane (PEGS) Solvent for
774 Precombustion CO2 Capture. The Journal of Physical Chemistry C 120, 20158-20169.

775 Shi, W., Siefert, N.S., Morreale, B.D., 2015. Molecular Simulations of CO2, H2, H2O, and H2S
776 Gas Absorption into Hydrophobic Poly(dimethylsiloxane) (PDMS) Solvent: Solubility and
777 Surface Tension. The Journal of Physical Chemistry C 119, 19253-19265.

778 Shi, W., Thompson, R.L., Macala, M.K., Resnik, K., Steckel, J.A., Siefert, N.S., Hopkinson,
779 D.P., 2019. Molecular Simulations of CO2 and H2 Solubility, CO2 Diffusivity, and Solvent
780 Viscosity at 298 K for 27 Commercially Available Physical Solvents. Journal of Chemical &
781 Engineering Data 64, 3682-3692.

782 Shi, W., Tiwari, S.P., Thompson, R.L., Culp, J.T., Hong, L., Hopkinson, D.P., Smith, K., Resnik,
783 K., Steckel, J.A., Siefert, N.S., 2021. Computational Screening of Physical Solvents for CO2
784 Pre-combustion Capture. The Journal of Physical Chemistry B 125, 13467-13481.

785 Siefert, N., Hopkinson, D., 2018. A High Performance Physical Solvent for Pre-Combustion
786 CO2 Capture, 2018 NETL CO2 Capture Technology Project Review Meeting, Pittsburgh, USA.

787 Siefert, N., Narburgh, S., Chen, Y., 2016a. Comprehensive Exergy Analysis of Three IGCC
788 Power Plant Configurations with CO2 Capture. Energies 9, 669.

789 Siefert, N.S., Agarwal, S., Shi, F., Shi, W., Roth, E.A., Hopkinson, D., Kusuma, V.A.,
790 Thompson, R.L., Luebke, D.R., Nulwala, H.B., 2016b. Hydrophobic physical solvents for pre-
791 combustion CO2 capture: Experiments, computational simulations, and techno-economic
792 analysis. International Journal of Greenhouse Gas Control 49, 364-371.

793 Smith, K., Ghosh, U., Khan, A., Simioni, M., Endo, K., Zhao, X., Kentish, S., Qader, A.,
794 Hooper, B., Stevens, G., 2009. Recent developments in solvent absorption technologies at the
795 CO2CRC in Australia. Energy Procedia 1, 1549-1555.

796 Smith, K.H., Anderson, C.J., Tao, W., Endo, K., Mumford, K.A., Kentish, S.E., Qader, A.,
797 Hooper, B., Stevens, G.W., 2012. Pre-combustion capture of CO2—Results from solvent
798 absorption pilot plant trials using 30wt% potassium carbonate and boric acid promoted
799 potassium carbonate solvent. International Journal of Greenhouse Gas Control 10, 64-73.

800 Smith, K.H., Ashkanani, H.E., Morsi, B.I., Siefert, N.S., 2022. Physical solvents and techno-
801 economic analysis for pre-combustion CO2 capture: A review. International Journal of
802 Greenhouse Gas Control 118.

Thompson, R.L., Culp, J., Tiwari, S.P., Basha, O., Shi, W., Damodaran, K., Resnik, K., Siefert, N., Hopkinson, D., 2019. Effect of Molecular Structure on the CO2 Separation Properties of Hydrophobic Solvents Consisting of Grafted Poly Ethylene Glycol and Poly Dimethylsiloxane Units. Energy and Fuels 33, 4432-4441.

Trapp, C., de Servi, C., Casella, F., Bardow, A., Colonna, P., 2015a. Dynamic modelling and validation of pre-combustion CO2 absorption based on a pilot plant at the Buggenum IGCC power station. International Journal of Greenhouse Gas Control 36, 13-26.

Trapp, C., Thomaser, T., Van Dijk, H.A.J., Colonna, P., 2015b. Design optimization of a pre-combustion CO2 capture plant embedding experimental knowledge. Fuel 157, 126-139.

Wu, T., 2022. National Carbon Capture Center (FE0022596), 2022 Carbon Management Project Review Meeting. National Energy Technology Laboratory, Pittsburgh, USA.

9 Supplemental Information

The following tables contain additional simulation detail, simulation results and experimental data including the raw data collected during VLE experiments and pilot plant trials. These VLE data were used to plot the figures in the main manuscript. The binary interaction parameters used for predicting gas solubility in the solvents in Aspen Plus via the PC-SAFT equation of state have also been provided. Simulation results for variation in solvent flow rate have also been provided.

Table S1. Equilibrium CO_2 solubility as a function of pressure and temperature for dry physical solvents (a) PEGDME, (b) CASSH-1, (c) PEG-PDMS-3, (d) TBP. These data were measured using the Hiden IGA VLE apparatus.

PEGDME CO_2 solubility, mol/L				
Temperature, °C → / **Pressure (MPa) ↓**	**10°C**	**25°C**	**40°C**	**55°C**
0	0	0	0	0
0.1	0.19	0.14	0.11	0.08
0.15	0.29	0.20	0.15	0.11
0.3	0.60	0.42	0.31	0.23
0.45	0.92	0.64	0.47	0.34
0.6	1.26	0.86	0.64	0.47
0.75	1.62	1.09	0.81	0.59
0.9	1.99	1.34	0.98	0.71
1.05	2.39	1.59	1.15	0.84
1.2	2.80	1.85	1.33	0.97
1.35	3.24	2.11	1.52	
1.5	3.70	2.39	1.70	
1.65	4.20	2.68	1.90	
1.8	4.72	2.98	2.10	
CASSH-1 CO_2 solubility, mol/L				
Temperature, °C → / **Pressure (MPa) ↓**	**10°C**	**25°C**	**40°C**	**55°C**
0	0	0	0	0
0.1	0.159	0.123	0.095	0.076
0.15	0.239	0.178	0.142	0.116
0.3	0.496	0.375	0.290	0.236
0.45	0.766	0.569	0.439	0.348
0.6	1.049	0.770	0.588	0.462
0.75	1.346	0.974	0.738	0.578

0.9	1.659	1.188	0.898	0.696
1.05	1.987	1.408	1.061	0.819
1.2	2.334	1.637	1.230	0.945
1.35	2.700	1.872	1.399	1.070
1.5	3.084	2.114	1.573	1.197
1.65	3.495	2.366	1.751	1.326
1.8	3.932	2.626	1.931	1.456
PEG-PDMS-3 CO_2 solubility, mol/L				
Temperature, °C → / **Pressure (MPa) ↓**	**10°C**	**25°C**	**40°C**	**55°C**
0	0	0.000	0	0
0.1	0.169	0.119	0.088	0.072
0.15	0.254	0.179	0.133	0.109
0.3	0.508	0.356	0.266	0.216
0.45	0.769	0.540	0.397	0.326
0.6	1.037	0.727	0.534	0.431
0.75	1.319	0.915	0.670	0.535
0.9	1.609	1.112	0.808	0.642
1.05	1.914	1.314	0.952	0.751
1.2	2.229	1.524	1.101	0.862
1.35	2.559	1.737	1.244	0.969
1.5	2.904	1.958	1.399	1.095
1.65	3.271	2.186	1.556	1.208
1.8	3.659	2.422	1.717	1.330
TBP CO_2 solubility, mol/L				
Temperature, °C → / **Pressure (MPa) ↓**	**10°C**	**25°C**	**40°C**	**55°C**
0	0	0	0	0
0.1	0.184	0.126	0.106	0.078
0.15	0.275	0.188	0.151	0.122
0.3	0.540	0.380	0.299	0.231
0.45	0.818	0.579	0.448	0.342
0.6	1.110	0.784	0.601	0.462
0.75	1.415	0.994	0.756	0.576
0.9	1.739	1.213	0.915	0.694
1.05	2.076	1.442	1.082	0.818
1.2	2.434	1.679	1.251	0.939
1.35	2.813	1.922	1.422	1.066
1.5	3.219	2.183	1.602	1.195
1.65	3.648	2.460	1.789	1.320
1.8	4.115	2.720	1.970	1.457

Table S2. Equilibrium pure gas solubility for CH_4, N_2 and H_2 as a function of pressure and temperature for dry physical solvents (a) PEGDME, (b) CASSH-1, (c) PEG-PDMS-3, (d) TBP. These data were measured using the CSTR apparatus. These data are not presented in figures in the manuscript.

PEGDME H_2 solubility			
25 ℃		40 ℃	
Pressure (Mpa)	**H_2 Solubility (mol/L)**	**Pressure (Mpa)**	**H_2 Solubility (mol/L)**
0.5038	0. 0052	0.5043	0.0049
1.1274	0.0240	1.1345	0.0213
1.7913	0.0439	1.8044	0.0387
2.4693	0.0645	2.4769	0.0567
2.9339	0.0777	2.9363	0.0682
CASSH-1 H_2 solubility			
25 ℃		40 ℃	
Pressure (Mpa)	**H_2 Solubility (mol/L)**	**Pressure (Mpa)**	**H_2 Solubility (mol/L)**
0.51	0.0083	0.51	0.0086
1.10	0.0201	1.10	0.0241
1.74	0.0336	1.74	0.0408
2.39	0.0464	2.39	0.0568
2.87	0.0571	2.87	0.0681
CASSH-1 N_2 solubility			
25 ℃		40 ℃	
Pressure (Mpa)	**N_2 Solubility (mol/L)**	**Pressure (Mpa)**	**N_2 Solubility (mol/L)**
0.49	0.0151	0.52	0.0168
1.05	0.0353	1.08	0.0380
1.67	0.0564	1.70	0.0589
2.32	0.0783	2.36	0.0791
2.79	0.0924	2.82	0.0958
CASSH-1 CH_4 solubility			
25 ℃		40 ℃	
Pressure (Mpa)	**CH_4 Solubility (mol/L)**	**Pressure (Mpa)**	**CH_4 Solubility (mol/L)**
0.45	0.0615	0.46	0.0570
1.01	0.1362	1.00	0.1239
1.64	0.2162	1.62	0.1977
2.29	0.2965	2.27	0.2676

2.78	0.3571	2.75	0.3193
PEG-PDMS-3 H_2 solubility			
25 ℃		40 ℃	
Pressure (Mpa)	**H_2 Solubility (mol/L)**	**Pressure (Mpa)**	**H_2 Solubility (mol/L)**
0.49	0.0094	0.48	0.0124
1.09	0.0214	1.09	0.0254
1.74	0.0342	1.74	0.0388
2.40	0.0482	2.40	0.0538
2.87	0.0576	2.87	0.0633
PEG-PDMS-3 N_2 solubility			
25 ℃		40 ℃	
Pressure (Mpa)	**N_2 Solubility (mol/L)**	**Pressure (Mpa)**	**N_2 Solubility (mol/L)**
0.4866	0.0121	0.4889	0.0235
1.0712	0.0366	1.0776	0.0477
1.7224	0.0653	1.7013	0.0747
2.3507	0.0984	2.3471	0.1060
2.8566	0.1261	2.8655	0.1328
PEG-PDMS-3 CH_4 solubility			
25 ℃		40 ℃	
Pressure (Mpa)	**CH_4 Solubility (mol/L)**	**Pressure (Mpa)**	**CH_4 Solubility (mol/L)**
0.4667	0.0617	0.4904	0.0606
1.0307	0.1428	1.0508	0.1362
1.6396	0.2363	1.6638	0.2175
2.2805	0.3440	2.3067	0.3066
2.7695	0.4230	2.7969	0.3765

Table S3. Equilibrium gas solubility at 25℃ as a function of pressure for dry physical solvents PEGDME, CASSH-1, PEG-PDMS-3 and TBP. These data were measured using the Isosorp VLE apparatus.

PEGDME at 25℃				
Pressure, MPa	**CO_2 solubility, mol/L**	**N_2 solubility, mol/L**	**H_2 solubility, mol/L**	**CH_4 solubility, mol/L**
0.1	0.14	0.0021	0.0021	0.0102
0.5	0.70	0.0106	0.0104	0.0511
1	1.49	0.021	0.021	0.1012
1.5	2.38	0.0317	0.0312	0.1501
2	3.38	0.0423	0.0416	0.1979

2.5	4.51	0.0528	0.0521	0.2447
3	5.79	0.0634	0.0625	0.2903
CASSH-1 at 25°C				
Pressure, MPa	**CO_2 solubility, mol/L**	**N_2 solubility, mol/L**	**H_2 solubility, mol/L**	**CH_4 solubility, mol/L**
0.1	0.1294	0.0038	0.0026	0.0167
0.5	0.6347	0.0188	0.0132	0.0829
1	1.3353	0.0377	0.0264	0.1634
1.5	2.1210	0.0565	0.0396	0.2415
2	3.0023	0.0753	0.0528	0.3173
2.5	3.9907	0.0942	0.0660	0.3909
3	5.0994	0.1130	0.0792	0.4622
PEG-PDMS-3 at 25°C				
Pressure, MPa	**CO_2 solubility, mol/L**	**N_2 solubility, mol/L**	**H_2 solubility, mol/L**	**CH_4 solubility, mol/L**
0.1	0.11	0.0034	0.0026	0.0146
0.5	0.57	0.0168	0.0130	0.0731
1	1.20	0.0331	0.0259	0.1453
1.5	1.91	0.0490	0.0389	0.2165
2	2.69	0.0645	0.0519	0.2869
2.5	3.56	0.0795	0.0648	0.3563
3	4.54	0.0940	0.0778	0.4248
TBP at 25°C				
Pressure, MPa	**CO_2 solubility, mol/L**	**N_2 solubility, mol/L**	**H_2 solubility, mol/L**	**CH_4 solubility, mol/L**
0.1	0.13	0.0041	0.0035	0.0177
0.5	0.65	0.0203	0.0173	0.0882
1	1.38	0.0403	0.0345	0.1751
1.5	2.21	0.0601	0.0518	0.2607
2	3.15	0.0797	0.0690	0.3450
2.5	4.22	0.0990	0.0863	0.4281
3	5.44	0.1181	0.1036	0.5098

Table S4. Equilibrium CO_2 gas solubility at 10, 25 & 40°C as a function of pressure for dry physical solvents PEGDME, CASSH-1, PEG-PDMS-3 and TBP. These data were measured using the Isosorp VLE apparatus.

PEGDME CO_2 solubility					
10 °C		**25 °C**		**40 °C**	
Pressure (Mpa)	**CO_2 Solubility (mol/L)**	**Pressure (Mpa)**	**CO_2 Solubility (mol/L)**	**Pressure (Mpa)**	**CO_2 Solubility (mol/L)**
0.1	0.22	0.1	0.14	0.1	0.10
0.5	0.99	0.5	0.70	0.5	0.51
1	2.16	1	1.49	1	1.06
1.5	3.65	1.5	2.38	1.5	1.66

2	5.53	2	3.38	2	2.30
2.5	7.91	2.5	4.51	2.5	3.00
3	10.92	3	5.79	3	3.75
CASSH-1 CO_2 solubility					
10 ℃		**25 ℃**		**40 ℃**	
Pressure (Mpa)	**CO_2 Solubility (mol/L)**	**Pressure (Mpa)**	**CO_2 Solubility (mol/L)**	**Pressure (Mpa)**	**CO_2 Solubility (mol/L)**
0.10	0.16	0.10	0.09	0.10	0.09
0.49	0.91	0.29	0.37	0.49	0.47
1.00	1.97	0.49	0.63	0.99	0.97
1.49	3.22	1.00	1.32	1.49	1.52
1.99	4.75	1.49	2.12	1.99	2.10
2.50	6.77	2.00	2.97	2.49	2.72
3.00	9.66	2.49	3.98	3.00	3.57
		1.49	2.13		
		0.51	0.65		
PEG-PDMS-3 CO_2 solubility					
10 ℃		**25 ℃**		**40 ℃**	
Pressure (Mpa)	**CO_2 Solubility (mol/L)**	**Pressure (Mpa)**	**CO_2 Solubility (mol/L)**	**Pressure (Mpa)**	**CO_2 Solubility (mol/L)**
0.1	0.18	0.1	0.11	0.1	0.08
0.5	0.81	0.5	0.57	0.5	0.43
1	1.75	1	1.20	1	0.89
1.5	2.90	1.5	1.91	1.5	1.38
2	4.30	2	2.69	2	1.91
2.5	6.01	2.5	3.56	2.5	2.47
3	8.09	3	4.54	3	3.07
TBP CO_2 solubility					
10 ℃		**25 ℃**		**40 ℃**	
Pressure (Mpa)	**CO_2 Solubility (mol/L)**	**Pressure (Mpa)**	**CO_2 Solubility (mol/L)**	**Pressure (Mpa)**	**CO_2 Solubility (mol/L)**
0.1	0.18	0.1	0.13	0.1	0.09
0.5	0.80	0.5	0.65	0.5	0.49
1	1.79	1	1.38	1	1.01
1.5	3.09	1.5	2.21	1.5	1.59
2	4.78	2	3.15	2	2.21
2.5	7.00	2.5	4.22	2.5	2.89
3	9.91	3	5.44	3	3.62

839

840

Table S5a. Inlet syngas composition data for each day of operation during trial 2 (Days 1-5: CASSH-1; Days 6-10: PEGDME). These normalized values represent averages from the two gas analyzers on each gas stream.

Syngas component	PEGDME					CASSH-1				
	Day 1	Day 1	Day 2	Day 3	Day 4	Day 5	Day 2	Day 3	Day 4	Day 5
H_2, mol%	15.0	17.8	15.0	15.8	16.9	16.9	13.8	14.1	16.0	16.2
N_2, mol%	28.0	23.9	26.0	23.6	22.1	25.3	28.4	25.2	27.1	24.0
CO, mol%	1.1	0.3	0.6	0.9	1.0	1.1	1.5	1.4	1.3	1.5
CO_2, mol%	53.9	55.2	56.3	57.0	57.5	54.5	53.6	56.9	53.1	55.7
CH_4, mol%	1.6	2.4	1.6	2.3	2.2	1.8	2.4	2.0	2.3	2.4
H_2S, ppm	3773.3	4188.8	4628.4	4107.8	4191.5	3951.0	3684.0	3529.2	2996.9	3067.4

Table S5b. Sweet gas composition data for each day of operation during trial 2. These normalized values represent averages from the two gas analyzers on each gas stream.

Sweet gas component	PEGDME					CASSH-1				
	Day 1	Day 1	Day 2	Day 3	Day 4	Day 5	Day 2	Day 3	Day 4	Day 5
H_2, mol%	33.4	35.6	32.0	37.5	36.3	34.8	34.0	33.4	37.5	38.1
N_2, mol%	58.4	52.2	60.2	51.7	53.4	54.2	59.3	58.5	53.3	52.4
CO, mol%	1.6	0.4	0.5	1.0	1.2	1.8	1.6	1.5	1.9	2.0
CO_2, mol%	2.2	6.3	4.1	5.5	4.4	4.2	1.7	1.8	1.7	1.6
CH_4, mol%	4.5	5.4	3.2	4.3	4.7	5.1	3.5	4.7	5.6	6.0
H_2S, ppm	99.2	150.9	173.6	164.8	161.5	167.3	114.7	111.0	113.8	108.1

Table S5c. Acid gas composition data for each day of operation during trial 2. These normalized values represent averages from the two gas analyzers on each gas stream.

Acid gas component	PEGDME					CASSH-1				
	Day 1	Day 1	Day 2	Day 3	Day 4	Day 5	Day 2	Day 3	Day 4	Day 5
H_2, mol%	0.2	0.4	0.3	0.4	0.4	0.4	0.2	0.2	0.2	0.3
N_2, mol%	2.5	2.6	3.0	2.7	2.7	3.1	2.7	2.5	2.3	2.2
CO, mol%	0.2	0.1	0.1	0.2	0.2	0.2	0.4	0.4	0.2	0.3
CO_2, mol%	95.8	95.2	95.1	95.2	95.2	94.7	95.3	95.4	95.8	95.7
CH_4, mol%	0.7	1.0	0.6	0.8	0.8	0.9	0.7	0.9	0.9	1.0
H_2S, ppm	6457.5	7673.6	8054.2	7213.1	7210.9	7151.5	6718.4	6075.9	5600.3	5477.3

Table S6. Process simulation predictions for water solubility during pilot plant operation for CASSH-1 and PEGDME before and after the flash process. Note that experimental water VLE data were not regressed into the process simulation.

	PEGDME		CASSH-1	
	Aspen Plus – Rate Based	**Aspen Plus - Equilibrium**	**Aspen Plus – Rate Based**	**Aspen Plus - Equilibrium**
Water Content Before Flash (ppm)	286	273	153	149
Water Content After Flash (ppm)	206	193	61	58
Experimental Water Content After Flash after Day 5 (ppm)	837		358	

Table S7. Computational predictions of CO_2 solubility in CASSH-1 from (Shi et al., 2021) at 10°C and 25°C

CASSH-1 at 10°C		CASSH-1 at 25°C	
Pressure, MPa	**Predicted CO_2 solubility, mol/L**	**Pressure, MPa**	**Predicted CO_2 solubility, mol/L**
0.125	0.060 ± 0.004	0.18	0.046 ± 0.003
0.25	0.113 ± 0.005	0.41	0.099 ± 0.004
0.5	0.230 ± 0.007	0.92	0.197 ± 0.006
0.7	0.307 ± 0.008	1.11	0.229 ± 0.006
		2.32	0.383 ± 0.008
		3.8	0.50 ± 0.01
		5.8	0.608 ± 0.006

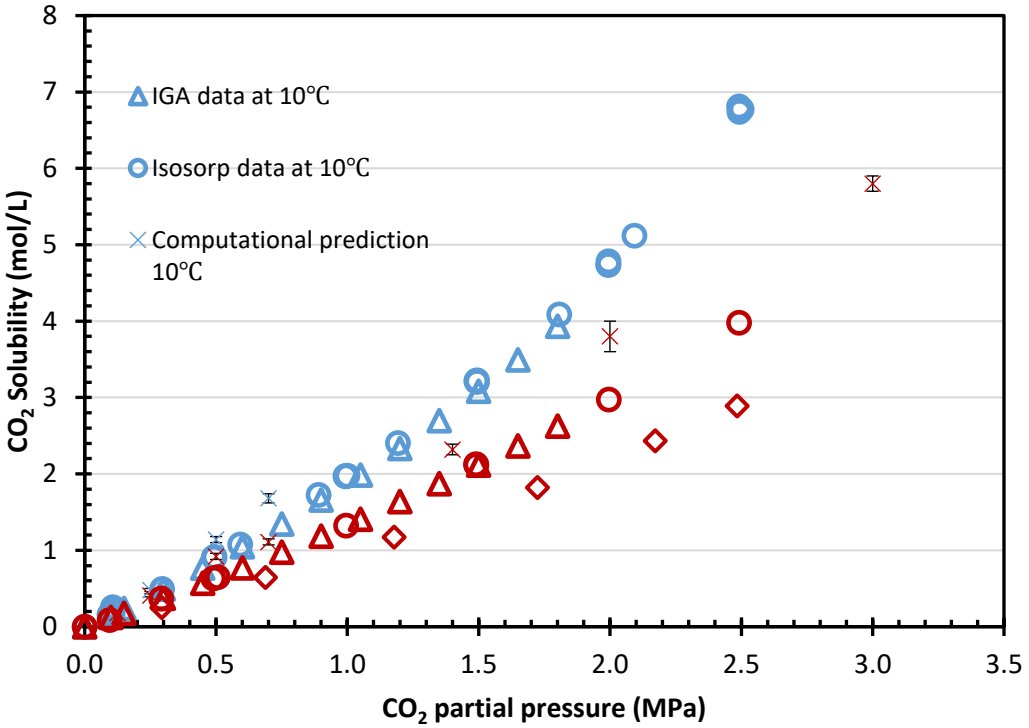

Figure S1. CO_2 solubility in CASSH-1 as a function of CO_2 partial pressure for experimental VLE data and computational predictions by Shi et al. (Shi et al., 2021)

Table S8. Binary interaction parameters for PC-SAFT equation of state used to predict gas solubility in solvents. The binary interaction parameters were predicted using the equation:

$$k_{ij} = A + \frac{B}{T'} + C \ln T' + DT' + ET'^2 \text{ where } T' = T/T_{ref}$$

The coefficients A, B, C, D and E in this equation are given in Table S8.

Component i	Component j	Regression	Temp units	A	B	C	D	E	Tref
CH_4	CO_2	APV110 PC-SAFT	K	0.065	0	0	0	0	298.15
CASSH-1	CO_2	USER	K	-0.0494	0	0	0.0994	0	298.15
CASSH-1	H_2	USER	K	-0.3	0	0	0	0	298.15
CASSH-1	N_2	USER	K	0.075	0	0	0	0	298.15
CASSH-1	CH_4	USER	K	-0.005	0	0	0	0	298.15
PEGDME	CO_2	USER	K	-0.07438	0	0	0.099383	0	298.15
PEGDME	H_2	USER	K	0.12	0	0	0	0	298.15
PEGDME	N_2	USER	K	0.25	0	0	0	0	298.15
PEGDME	CH_4	USER	K	0.122	0	0	0	0	298.15

Table S9. Process simulation results for variation in solvent flow rate (Q_s) (avg. $Q_s \pm 1\sigma$ = average solvent flow rate ± 1 standard deviation). These simulation results were obtained using the Aspen Plus rate based model using operating conditions found in Table 3 (and varying solvent flow rates as shown below) and the process flow sheet found in Figure 2.

Solvent:	**PEGDME**			**CASSH-1**		
Property	**Pilot plant**	**Simulation**		**Pilot plant**	**Simulation**	
	Q_S avg. = 32.0 L/h	**$Q_S + 1\sigma$ = 33.7 L/h**	**$Q_S - 1\sigma$ = 29.9 L/h**	**Q_S, avg. = 32.4 L/h**	**$Q_S + 1\sigma$ = 34.3 L/h**	**$Q_S - 1\sigma$ = 30.1 L/h**
Absorber temperature						
Top of column	24.9 ± 0.3	25.3	25.5	28.7 ± 1.3	24.81	25.09
Upper	25.5 ± 0.7	26.3	26.8	34.0 ± 1.5	25.71	26.62
Mid	26.7 ± 1.6	27.8	28.9	37.7 ± 1.1	27.31	29.01
Lower	30.1 ± 2.8	30.4	31.9	39.6 ± 0.7	29.91	32.19
Bottom of column	36.4 ± 2.0	34.2	35.8	40.0 ± 0.6	33.41	35.30
Sweet gas flow rate, mol/h	59.3 ± 1.0	67.0	69.5	67.1 ± 5.2	66.5	70.6
Sweet gas, mol%						
H_2	36.5 ± 1.0	31.8	30.8	35.0 ± 2.1	35.4	33.7
N_2	55.4 ± 1.0	55.7	54.0	54.6 ± 1.5	53.9	51.4
CO	1.73 ± 0.04	1.9	1.9	1.1 ± 0.1	1.5	1.4
CO_2	1.6 ± 0.2	7.4	10.1	5.1 ± 0.3	6.9	11.1
CH_4	4.9 ± 0.1	3.2	3.1	4.2 ± 0.3	2.4	2.3
H_2S	0.012 ± 0.001	0.006	0.006	0.017 ± 0.001	0.01	0.01
Acid gas flow rate, mol/h	85.0 ± 1.0	78.3	75.8	81.3 ± 3.3	83.1	79.0
Acid gas, mol%						
H_2	0.21 ± 0.04	1.2	1.1	0.45 ± 0.15	1.6	1.4
N_2	2.6 ± 0.2	2.3	2.1	3.2 ± 0.40	3.5	3.1
CO	0.25 ± 0.05	0.32	0.29	0.14 ± 0.10	0.09	0.08
CO_2	95.6 ± 0.2	94.9	95.3	94.6 ± 0.30	93.4	94.1
CH_4	0.78 ± 0.10	0.56	0.51	0.82 ± 0.08	0.66	0.58
H_2S	0.60 ± 0.05	0.63	0.65	0.74 ± 0.01	0.74	0.77
CO_2 recovery, %	99.0 ± 0.5	94	91	95 ± 5	94	90
CO_2 uptake, mol×L^{-1}	2.49 ±0.06± 0.15	2.20	2.41	2.40 ±0.13± 0.14	2.26	2.47